POSEIDON WATER

Appendix BB
Revised Hydrodynamic Discharge Modeling Report

Renewal of NPDES CA0109223
Carlsbad Desalination Project

Note on the Zone of Initial Dilution in a Quiescent Ocean Due to Discharges of Concentrated Seawater from the Carlsbad Desalination Project

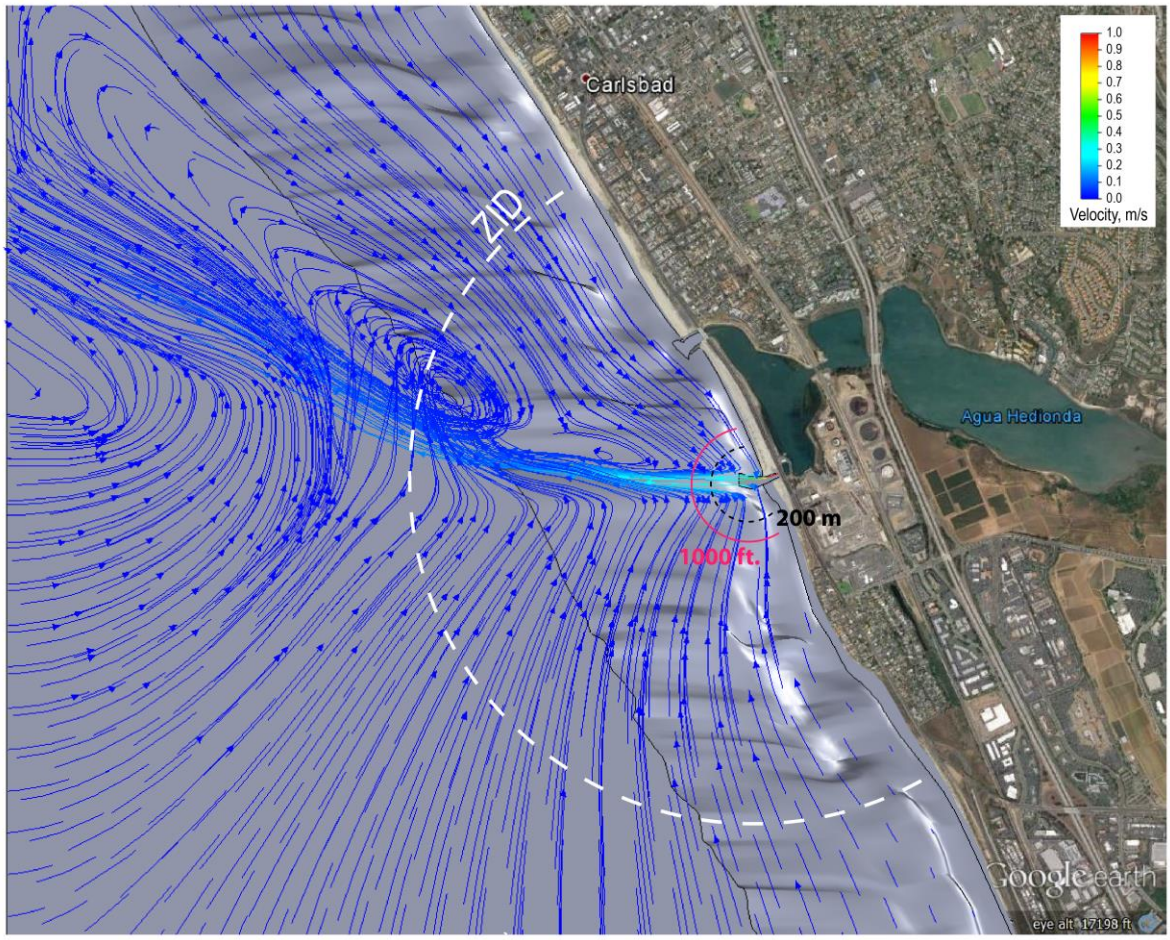

Submitted by:
Scott A. Jenkins, Ph.D.
Technical Manager, Coastal Sciences & Engineering
Michael Baker International

Submitted to:
Poseidon Water LLC
5780 Fleet Street, Suite 140
Carlsbad, CA 92008

Draft: 2 April 2016; First Revision 6 April 2016; Second Revision 18 June 2016;
Final: 12 July 2016

ABSTRACT: A set of coupled high resolution dilution models were constructed and run to resolve initial dilution of concentrated seawater and trace pollutants at the boundaries of the zone of initial dilution (ZID) under stand-alone operations of the Carlsbad Desalination Project (CDP). Peer reviewed, published and USEPA certified hydrodynamic models were employed to resolve initial dilution and discharge plume trajectories under standard NPDES dilution modeling protocols (as defined in the California Ocean Plan); according to which "*Initial Dilution will be considered the process which results in the rapid and irreversible turbulent mixing of wastewater with ocean water around the point of discharge".* As such the models do not consider any additional mixing due to the action of ocean currents, waves, tides or wind. The models were initialized for quiescent ocean receiving waters at mean sea level bounded by the existing beach and offshore bathymetry surrounding the discharge channel for the Carlsbad Desalination Project. The discharge channel was initialized in the models according to as-built drawings, thereby establishing the appropriate Manning's roughness coefficient that corresponds to the size of stone used in construction of the discharge jetties and discharge channel bottom. The models evaluate initial dilution for effluent discharge streams of 238 mgd with a salinity of 42 ppt in the discharge pond east of Carlsbad Blvd., prior to discharge into the shorezone through the discharge channel. Effluent discharge streams were assumed to be within a couple of degrees of ambient ocean temperature ($\Delta T = 0$ to $+ 2\ ^0C$) based on temperature monitoring data after 5 months of operations of the CDP. Ocean receiving waters were initialized with the monthly mean temperature and salinity profiles that result in a minimum initial dilution (minimum month). The minimum month was determined to be September 2008, the same minimum month scenario that was used for the recently renewed discharge permit for the nearby San Juan Creek Ocean Outfall (NPDES NO. CA0107417 ORDER NO. R9-2012-0012). Both the CDP and the San Juan Creek Ocean Outfall reside in the same littoral cell (the Oceanside Littoral Cell), and therefore consistency in using the same temperature/salinity depth profile to define worst-case is sensible. Initial dilution was considered to be complete along the loci of points in the receiving water where the gradient in dilution factor is less than 1%. Initial dilution was considered to have reached a steady state along that loci of points when the variance in dilution factor between two adjacent computational steps became less than 1%.

The matched CORMIX 5.0 and *COSMOS/ FLowWorks* model solutions of still water dilution of CDP brine discharge show that it flows downslope and offshore as a gravity flow, by exchanging potential energy in elevation for kinetic energy and following bottom depressions in the micro-bathymetry formed by a series of offshore sand-waves. These bottom depressions are skewed away from the shoreline-normal alignment, diverging towards the west-northwest and causing the trajectory of the brine plume to bend in that general direction as it follows the local bottom gradients. As the brine plume follows the troughs in the bathymetric sand waves, it creates a massive system of entrainment streams and eddies that also exhibit this same northwesterly bias away from shoreline-normal alignment. This is in direct contrast to the general behavior of the brine plumes modeled in the antecedent study (Jenkins and Wasyl, 2015), where the brine plumes consistently exhibit a southerly displacement due a prevailing southerly drift from tidal currents and wave-induced longshore currents. The large-scale

entrainment flow patterns and eddies in the quiescent ocean simulations would never exist in Nature, as these organized flow features would be sheared and broken up by shoaling waves and coastal boundary layer currents. The brine plume becomes stationary at distance of 1,851 m from the ends of the discharge jetties. At this point, the change in dilution factor D_m with distance offshore becomes less than 1%. The Ocean Plan defines the *zone of initial dilution* (ZID) as the zone in which the process of initial dilution is completed; and since dilution ceases to increase significantly beyond 1851 m from the point of discharge, this distance marks the seaward limit of the ZID. Initial dilution at the ZID reaches a robust dilution factor of $D_m = 52.1$ to 1 for a $\Delta T = 0\ ^0C$; increasing slightly to $D_m = 55.0$ to 1 for a $\Delta T = +2\ ^0C$. These determinations of Dm are based on an effluent concentration of 42 ppt in the discharge pond (compliance point M-002). We find that the salinity maxima decline to 2 ppt over natural background at a distance of 196 m from the point of discharge, where Dm = 3.25. At the 200 m BMZ boundary, the maxima in discharge salinity is 35.47 ppt, thereby satisfying the brine amendment of the California Ocean Plan, (Appendix-A of SWRCB 2015). The corresponding dilution factor is $D_m = 3.31$ at the BMZ 200 m boundary. This result is within the statistical spread of dilution results in the antecedent study when corrected for partially diluted brine as it leaves the discharge pond, (cf. Figure 18 in Jenkins and Wasyl, 2015). At the historic 1,000 ft radius ZID written in NPDES permits for Encina Power Station, maximum brine salinity is diluted to 34.9 ppt with a corresponding dilution $D_m = 5.07$ for a $\Delta T = 0\ ^0C$; and $D_m = 5.08$ for a $\Delta T = +2\ ^0C$. The weak sensitivity of dilution a great distance to Delta-T variance is due to the fact that the mass diffusivity of NaCl in water (a proxy for sea salts) increases moderately with increasing temperature, with $\Delta T = 0\ ^0C$ representing worst-case initial dilution. A tabular summary of discharge maximum salinity and minimum dilution factor values is found in Table ES-1 for intermediate distances from the point of discharge.

Mechanics of Initial Dilution of Brine: In the Ocean Plan the concept of when initial dilution is complete is also associated with when the momentum induced velocity of the discharge ceases to produce significant mixing of the waste. The heavy brine effluent initially has two components of momentum: 1) momentum in the velocity field (mass x velocity), and 2) momentum in the force field (force x time, or *impulsive momentum*); where the force field comes from gravity as a consequence of the negative buoyancy of the brine. As the brine begins to flow offshore and down the slopes of the nearshore bathymetry, momentum in the gravitational force field flows (*fluxes*) into the velocity field, and the brine accelerates under the force of gravity due to its negative buoyancy. Some of the gravitational acceleration is transferred to stresses of bottom friction, but the remaining momentum of the discharge stream is restructured as a system of entrainment streams and eddies, all of which derive their momentum and velocity from the initial discharge stream. The entrainment streams are *return flows* of receiving water that were displaced by the offshore-directed push (*momentum flux*) of the discharge stream, and transport receiving water into the ZID from offshore and from along-shore sources which eventually merge with the discharge stream to produce dilution. Eddies are produced by shear stresses between the discharge stream and the receiving water which transfer momentum of the discharge stream into eddy momentum (*vorticity*), producing *irreversible turbulent mixing*. The dilution action of the entrainment streams and eddies dilutes both the waste (brine) as well as the momentum contained in the discharge, until

at some point offshore, the discharge becomes neutrally buoyant and the momentum of the residual velocity field is so diluted that turbulent mixing ceases. That point marks the edge of the ZID, and can be inferred from the velocity field as the zone beyond which organized eddy motion ceases.

Table ES-1: Summary of minimum monthly dilution (Dm) as a function of distance from the point of discharge into the receiving water.

Distance from Discharge, (m)	Maximum Salinity of Discharge for $\Delta T = 0^0$ C, (ppt)	Maximum Salinity of Discharge for $\Delta T = +2^0$ C, (ppt)	*Dilution Factor, Dm, for $\Delta T = 0^0$ C	*Dilution Factor, Dm, for $\Delta T = +2^0$ C
0.00	42.000	42.000	0	0
10.78	40.956	40.956	0.14	0.14
21.07	39.528	39.485	0.41	0.42
50.19	37.435	37.435	1.16	1.16
54.90	37.311	37.294	1.23	1.24
73.17	36.807	36.794	1.57	1.58
100.0	36.381	36.371	1.95	1.96
110.0	36.233	36.232	2.11	2.11
120.0	36.131	36.130	2.23	2.23
130.0	36.060	36.059	2.32	2.32
140.0	35.956	35.949	2.46	2.47
150.0	35.901	35.894	2.54	2.55
160.0	35.760	35.754	2.76	2.77
170.0	35.685	35.679	2.89	2.90
180.0	35.614	35.609	3.02	3.03
190.0	35.543	35.538	3.16	3.17
196.0	35.502	35.495	3.25	3.26
200.0	35.472	35.467	3.31	3.32
264.0	35.100	35.097	4.31	4.32
328.1	34.900	34.898	5.07	5.08
600.0	34.420	34.419	8.23	8.24
1000	34.174	34.164	11.6	11.8
1300	34.011	33.994	16.0	16.2
1600	33.830	33.828	24.7	24.9
1800	33.700	33.698	41.4	41.9
1851	33.660	33.651	52.1	55.0
2000	33.621	33.618	69.8	71

*Based on 42 parts per thousand (ppt) effluent concentration at station M-002 (discharge pond)

Note on the Zone of Initial Dilution in a Quiescent Ocean Due to Discharges of Concentrated Seawater from the Carlsbad Desalination Project

By: Scott A. Jenkins, Ph.D.

1) Introduction:

This is a supplement to Jenkins and Wasyl (2015), "Hydrodynamic Dilution Analysis for the Carlsbad Desalination Project Operating at Sixty Million Gallons Per Day Production Rate". This previous study was a supporting document to the renewal application for NPDES permit # CA0109223 for the Carlsbad Desalination Project, (CDP) in which dilution of concentrated seawater discharged into the surfzone and nearshore receiving waters off Carlsbad CA was analyzed under worst-case ocean mixing conditions derived from the historic record of waves, currents, tides, and winds. The present supplemental hydrodynamic analysis has been conducted in response to requests form the Regional Water Quality Control Board, San Diego Region to perform an *initial dilution* analysis for a perfectly quiescent ocean, i.e., in the absence of any motion or mixing in the receiving waters due to waves, currents, tides, or winds. In particular, the present study is tasked with determining the relationship between the *Zone of Initial Dilution* (ZID) and the area within the *Brine Mixing Zone* (BMZ).

Under the newly amended *California Ocean Plan* as presented in Appendix-A of SWRCB (2105), a new numeric water quality objective has been established that limits brine discharges from ocean desalination plants (whose construction are 80% complete) to no more than 2 ppt over ambient ocean salinity (*natural background salinity*) at the outer edge of a BMZ measuring 200 m (656 ft) in radius around the point of discharge into the receiving waters. Under this new Ocean Plan amendment, *natural background salinity* is to be determined from 20 years of ocean salinity measurements representative of the at project site. The relationship between the ZID and the BMZ is evaluated for the maximum possible hyper-salinity impact, (per Table-1 NPDES CA0109223, RWQCB, 2105), arising when the desalination plant increases product water production capacity from 50 million gallons per day (mgd) to 60 mgd, and discharges 238 mgd of concentrated seawater (brine) at a salinity of 42 ppt in the discharge pond, (cf Figure 1).

2) Regulatory Definitions of Initial Dilution and the Zone of Initial Dilution:

Initial dilution is defined within Appendix I of the *California Ocean Plan* as follows:

> *Initial Dilution is the process which results in the rapid and irreversible turbulent mixing of wastewater with ocean water around the point of discharge.*
>
> *For a submerged buoyant discharge, characteristic of most municipal and industrial wastes that are released from the submarine outfalls, the momentum of the discharge and its initial buoyancy act together to produce turbulent mixing. Initial dilution in this case is completed when the diluting wastewater ceases to rise in the water column and first begins to spread horizontally.*
>
> *For shallow water submerged discharges, surface discharges, and nonbuoyant discharges, characteristic of cooling water wastes and some individual discharges, turbulent mixing results primarily from the momentum of discharge.*

Figure 1: Aerial view showing spatial relationship between the discharge pond located in the southwest corner of the Agua Hedionda Lagoon immediately east of Carlsbad Blvd. and the discharge channel bounded by a pair of jetties that terminate in the surf zone. (photo courtesy of NRG Energy).

> *Initial dilution, in these cases, is considered to be completed when the momentum induced velocity of the discharge ceases to produce significant mixing of the waste, or the diluting plume reaches a fixed distance from the discharge to be specified by the Regional Board, whichever results in the lower estimate for initial dilution.*

Here, non-buoyant discharges are those whose density matches that of the receiving water, and consequently have no net buoyancy. Brine is actually a buoyant discharge in which the buoyancy is negative. Brine dilution behaves like that from a municipal waste water outfall turned upside down; where instead of rising from the seabed toward the sea surface as treated wastewater effluent behaves, brine descends from near the sea surface and falls towards the seabed.

The California Ocean Plan only provides a notional definition the ZID as the zone in which the process of initial dilution is completed. The California Ocean Plan establishes receiving water concentration standards that are to be achieved upon completion of initial dilution. Provision III.C.4.d of the Ocean Plan states:

For the purpose of this Plan, minimum initial dilution is the lowest average initial dilution within any single month of the year. Dilution estimates shall be based on observed waste characteristics, observed receiving water density structure, and the assumption that no currents, of sufficient strength to influence the initial dilution process, flow across the discharge structure.

Provision III.M.3.b of the amended Ocean Plan (SWRCB, 2015) requires owners or operators of desalination facilities to develop a dilution factor (Dm) for application to the BMZ:

The dilution factor (Dm) shall be developed within the Brine Mixing Zone using applicable water quality models that have been approved by the regional water boards in consultation with State Water Board staff.

Under the terms within Appendix I of the *California Ocean Plan* the solution for the ZID boundary requires model input defined as, "*the trapping level when considering worst-case scenarios*". Trapping levels result from the vertical stratification of the receiving waters as a consequence of the temperature/salinity depth profile, and the worst case month results from the weakest degree of vertical stratification when temperature and salinity have the smallest gradient between the sea surface and the sea floor.

3) Technical Approach:

To convert the notional water quality definition of the ZID into a mathematical equation that the hydrodynamic model can solve, we pose the ZID definition as a *calculus of variations* problem, (Boas, 1966). Because the highest salinity in the discharge plume is found on the seabed, the ZID represents a closed contour curve ζ on the seabed surrounding the outfall along which the total momentum flux of the discharge plume reaches a *stationary minimum*. The curvilinear coordinate ζ that defines the ZID

contour may be written in model coordinates as,

$$d\zeta = \sqrt{(dx)^2 + (dy)^2} = \sqrt{1 + x'^2}\, dy = \sqrt{1 + y'^2}\, dx \qquad (1)$$

$$x' = \frac{dx}{dy} \quad ; \quad y' = \frac{dy}{dx}$$

where x is the model grid coordinate in longitude, and y is the grid coordinate in latitude. Gridding for the ZID modeling herein is by latitude and longitude with a 0.1 x 0.1 arc second grid cell resolution yielding a computational domain of 2 km x 2 km.

The momentum flux of the discharge plume has two components: 1) momentum in the velocity field, and 2) momentum in the force field; where the force field comes from gravity as a consequence of the negative buoyancy of the brine. The momentum flux of the discharge plume $H(\zeta)$, is written (Batchelor, 1970) as:

$$H(\zeta) = \frac{1 - c_f}{2}\, \rho_s\, u_s^2(\zeta) \quad + \quad \left[\rho(\zeta) - \rho\right] g\, h(\zeta) \qquad (2)$$

where $\rho_s(\zeta)$ is the density of the brine plume; ρ is ambient sea water density; $u_s(\zeta)$ is the fluid velocity in the discharge plume along the ζ contour; $h(\zeta)$ is the local depth along the ζ contour, and c_f is the bottom friction coefficient related to seabed roughness. The first term on the right hand side of equation-2 is the momentum flux due to the discharge velocity, while the second term is the momentum flux associated with the net buoyancy (negative) of the discharge plume. The variational problem for the ZID requires minimization of the integral:

$$\oint H(\zeta)\, d\zeta \quad \rightarrow \quad \text{stationary minimum} \qquad (3)$$

Because the plume by definition must be a stationary spreading front at the ZID contour, the velocity field term in equation-2 vanishes as the plume velocity decays to stagnation along the stationary front, ($u_s \rightarrow 0$). The force field term in equation-2 reaches a minimum wherein the density structure of the plume is in hydrostatic balance with the ambient ocean density field, ($\rho_s \rightarrow \rho$). This reduces the contour integral in equation-3 to the more tractable indefinite integral:

$$\oint H(\zeta)\, d\zeta = \int F(y, x, x')\, dy \qquad (4)$$

where:

$$F(y, x, x') = (\rho_s - \rho)\, g\, h\,(x, y)\, \sqrt{1 + x'^2}$$

The variational problem for the ZID can thus be posed in terms of finding the depth contour $h(x, y)$ that minimizes the integral on the right hand side of equation-4. This is accomplished by solving the *Euler-Lagrange equation* [*Boas*, 1966],

$$\frac{\mathrm{d}}{\mathrm{d}y}\frac{\partial F}{\partial x'} - \frac{\partial F}{\partial x} = 0 \qquad (5)$$

Equation-5 is solved by double integration using the hydrodynamic solutions for the discharge plume density field. The solution is based quiescent ocean receiving waters at mean sea level, with no waves, currents tides or wind mixing.

Analysis of brine dilution at the BMZ, initial dilution at the edge of the ZID and delineation of the ZID boundary itself is based on a combination of hydrodynamic models. It is standard practice to use a near-field dilution model for the initial dilution of the turbulent discharge, and a far-field dilution model for predicting the trajectory and dispersion of the discharge plume after initial dilution. The unique feature of the present problem is that the processes initial dilution and dispersion occur as a gravity flow on a sloping bottom. As the heavy brine effluent flows downslope from the discharge channel into the deeper receiving waters offshore, initial dilution is continually regenerated as this gravity flow converts potential energy of elevation into turbulent kinetic energy. Therefore initial dilution extends into the far-field and two separate types of models are required to fully resolve the initial dilution problem. For the near field mixing zone model, we employ CORMIX 5.0, certified by the U.S. Environmental Protection Agency and the California State Water Resources Control Board for use in ocean outfall design (Baumgartner, et al., 1994). For the far-field trajectory and dispersion solution we employ a class of models known as ***computational fluid dynamics*** (CFD). We used two different CFD models: 1) *COSMOS/ FLowWorks* was employed solve the far-field brine dispersion trajectories, and 2) the regeneration of turbulent kinetic energy from downslope flow was evaluated using a $\bar{v}^2 - f$ mode computational fluid dynamics model, *Star-CD ,* Version 3.1, with *QUICK* space discretization for the mean flow and first order up-winding of the turbulence equations, (Iaccarino, G, 2000, Star, 1998).

4) Model Initialization

The models were initialized for quiescent, tideless ocean receiving waters at mean sea level bounded by the existing beach and offshore bathymetry surrounding the discharge channel for the Carlsbad Desalination Project. The discharge channel was initialized in the model according to as-built drawings, thereby establishing the appropriate Manning's roughness coefficient in the model that corresponds to the size of stone used in construction of the discharge jetties and discharge channel bottom. The temperature and salinity profiles in the receiving water were initialized from historic monitoring of ocean water mass properties at the nearby Scripps Pier,(SIO, 2013), and from buoy moorings near the Carlsbad Submarine Canyon and Oceanside Pier deployed under the CDIP (2012) and CalCOFI, (2014) programs as archived by SCCOOS, (2014).

4.1) Bathymetry: Unlike the antecedent dilution study (Jenkins and Wasyl (2015), that used dynamic bathymetry that was interactive with ocean historic wave forcing, the present study uses rigid-boundary bathymetry referenced to mean sea level. This fixed bathymetry was obtained in 1 arc-second resolution from the National Geophysical Data Center http://maps.ngdc.noaa.gov/viewers/wcs-client/ using the Southern California Coastal Relief Model (1 arc-second)" layer. The data were then corrected in the very nearshore using a detailed set of post-dredging bathymetric surveys

that were measured by San Diego Gas and Electric Company (SDG&E) following the 1997-98 lagoon re-construction and maintenance dredging (Figure 2); and further refined using higher survey resolution by Ewany, et al., (1999), obtained in a study commissioned by the California Coastal Commission. The resulting depth contours were input to ARCGIS kriging algorithms to create a 3-dimensional CAD model of the seafloor off Agua Hedionda Lagoon, (Figure 3), thereby creating a farfield computational grid at 0.1 arc-second horizontal resolution and covering an area of receiving water 6 km x 6 km.

4.2) Salinity and Natural Background Definition: Figure 4 shows the variation in daily mean sea surface salinity in the coastal waters off the Carlsbad Desalination Project while Figure 5a a shows daily mean seafloor salinity, both plotted from 30 years of monitoring data derived from the archival data bases of Scripps Institution of Oceanography (Scripps Pier Shore Station, SIO, 2010) and the Coastal Data Information Program (CDIP, 2012), supplemented by site monitoring data from the SDG&E monitoring reports by MBC (2001-2015). The period of these unbroken archival sources extends from 1980 until March 2010. Daily mean values from these archival sources produced 11,017 data points. Inspection of Figures 4.4a & 4.5a indicate that the ocean salinity varies naturally by 10% between summer maximums and winter minimums, with a long term average value of 33.52 parts per thousand (ppt) on the surface and 33.49 ppt on the seafloor. Average sea surface salinity is slightly higher due to evaporation. Maximum salinity was 34.3 ppt on the sea surface and seafloor during the 1998 summer El Nino when southerly winds transported high salinity water from southern Baja up into the Southern California Bight. Minimum salinity was 31.06 ppt on the sea surface and 30.4 ppt on the seafloor during the 1992 floods. The variation between maximum and minimum salinity is about 3.2 ppt to 3.9 ppt, which is about 10 % of the depth-averaged value of 33.5 ppt.

N*atural background salinity* according to the amended Ocean Plan is a reference location that is representative of the *natural background salinity* of the discharge location. For the purposes of this evaluation, we have adopted the period of record at the Scripps Pier (SIO 2013) as the natural background salinity. Figure 6 plots the full 33 year period of record at the Scripps Peer Shore Station at
http://www-mlrg.ucsd.edu/shoresta/mnSIOMain/siomain.htm
The period of record, 1980 to 2013 contains 12,055 verified daily measurements. Monthly averages for each individual month in a 20-year reference period and the full 33-year period of record are given. The long-term mean for both the 20 and 30 year time frames are the same, 33.52 ppt; and monthly means vary by no more than 0.2 ppt about the long-term mean.

4.3) Ocean Temperature: The ocean temperature effects the buoyancy of the brine discharge through the absolute temperature of the discharge. This buoyancy effect is calculated by the specific volume change of the discharge relative to the ambient ocean water (see Appendix-1). The buoyancy of the brine plume exerts a strong effect on the mixing and rate of assimilation of the sea salts by the receiving waters. We use the average of temperature records from the archival databases of Scripps Institution of Oceanography (CalCofi, 2012) and the Coastal Data Information Program (CDIP, 2012). An 11,017 point record of daily mean sea surface temperatures are plotted in Figure 4b, while daily mean seafloor temperatures are plotted in Figure 5b. These temperature data

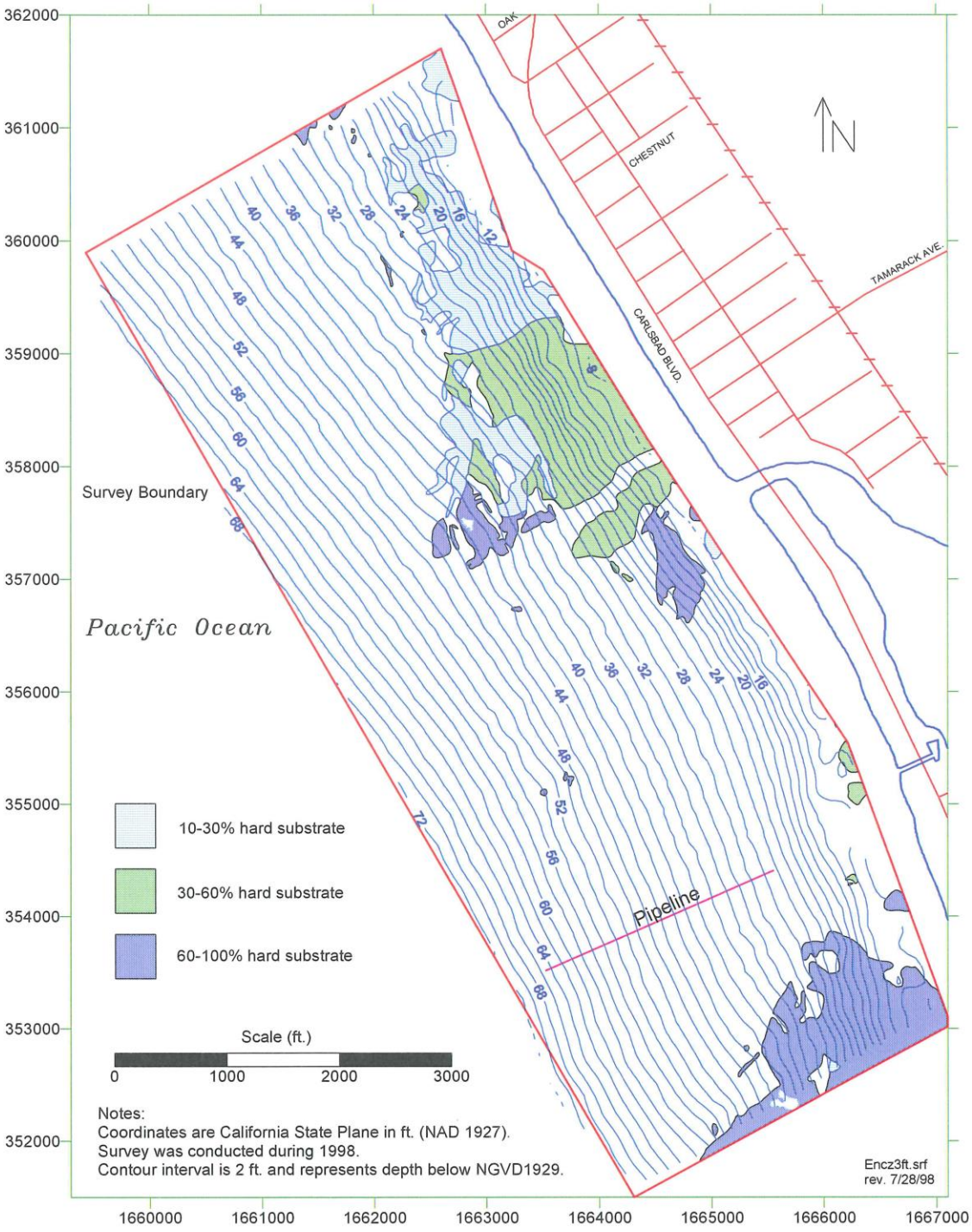

Figure 2: Bathymetry and substrate exposure in the vicinity of Agua Hedionda Lagoon, from Elwany et al., (1999).

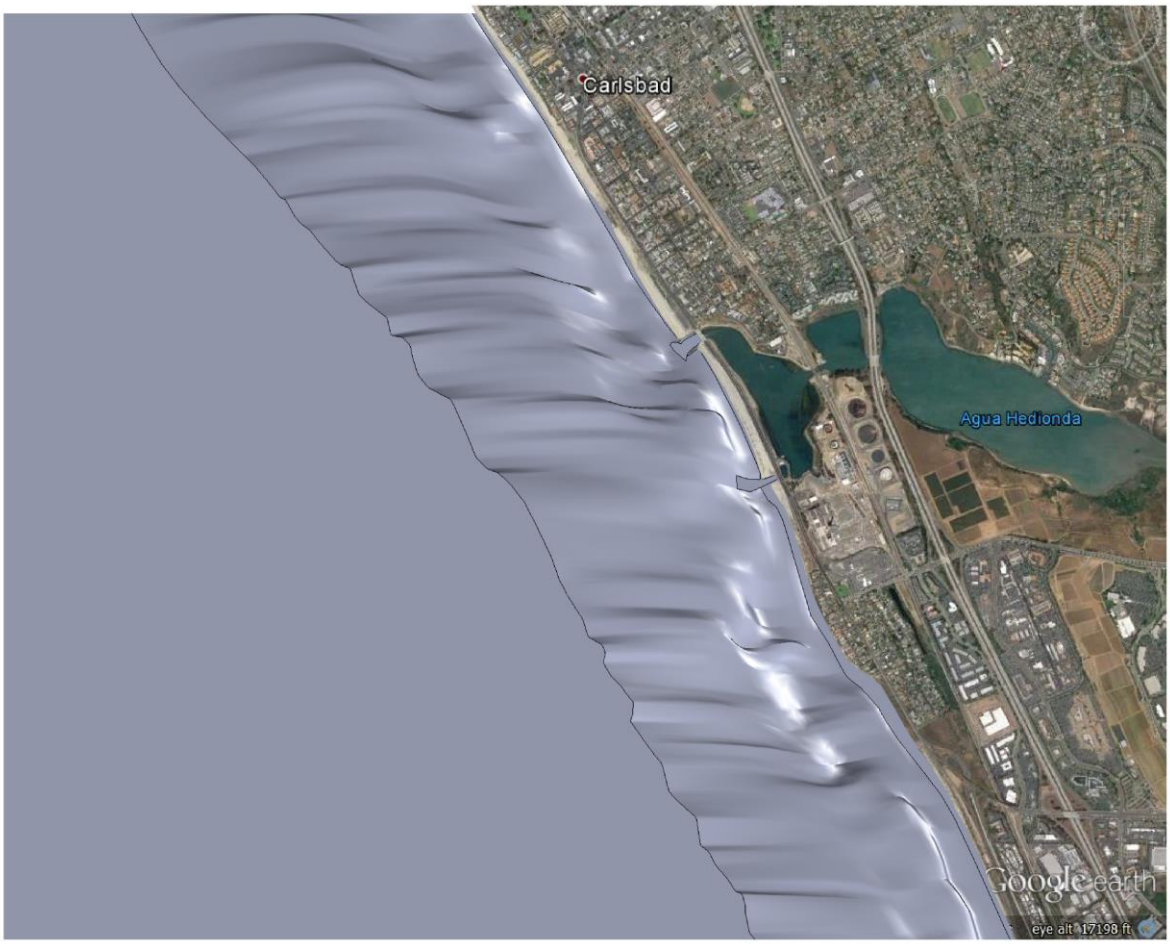

Figure 3: Three-dimensional CAD bathymetry creating a farfield computational grid at 0.1 arc-second horizontal resolution and covering an area of receiving water 6 km x 6 km in the vicinity of Agua Hedionda Lagoon. Intersection of trapping level with the seabed shown as black offshore contour

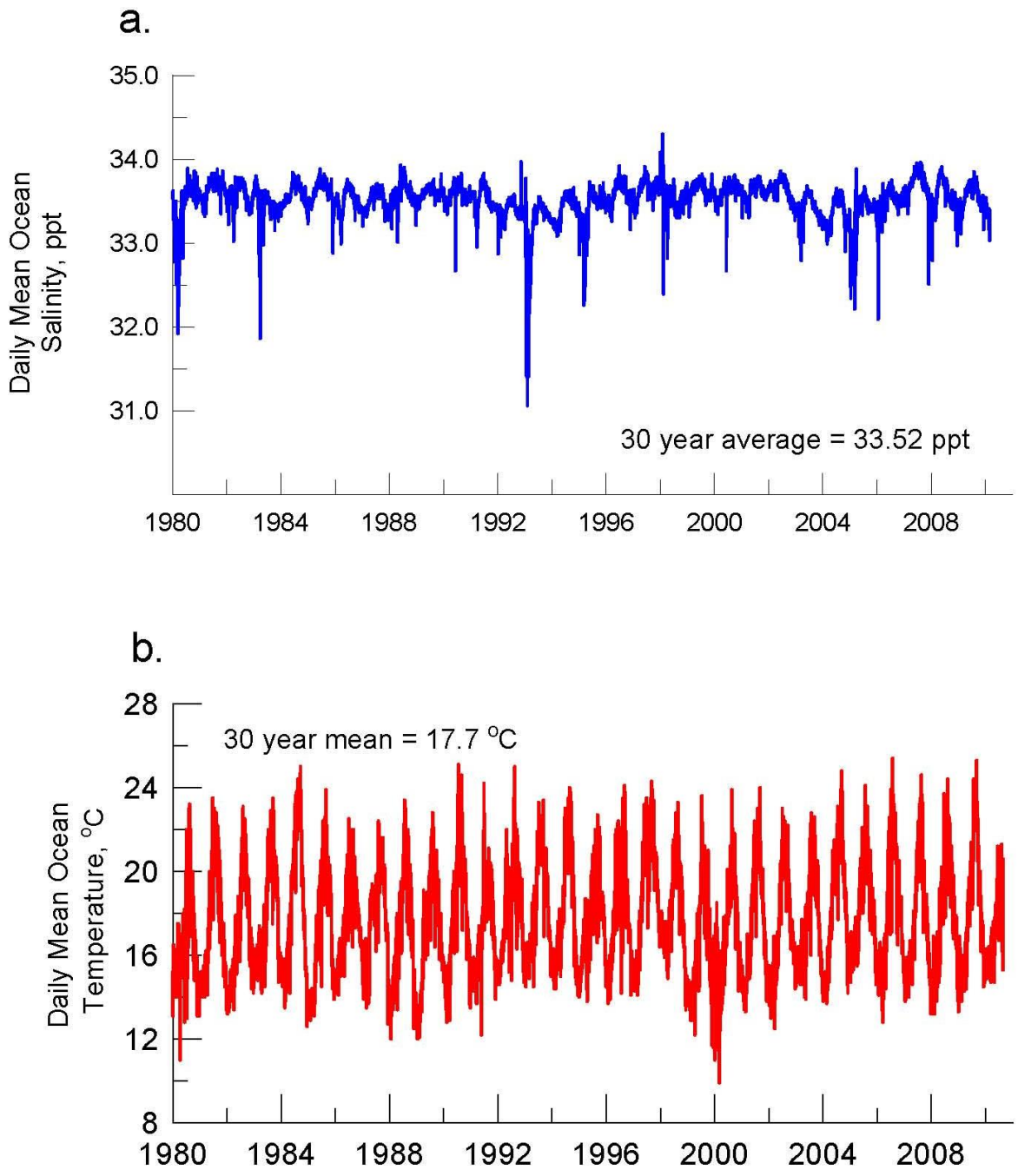

Figure 4: Daily mean ocean surface salinity (a) and daily mean ocean surface temperature (b) at the Carlsbad Desalination Project; from CDIP (2012), SIO, (2010), CalCOFI (2014) and NPDES/ CA0107417monitoring reports by MBC (2001-2015).

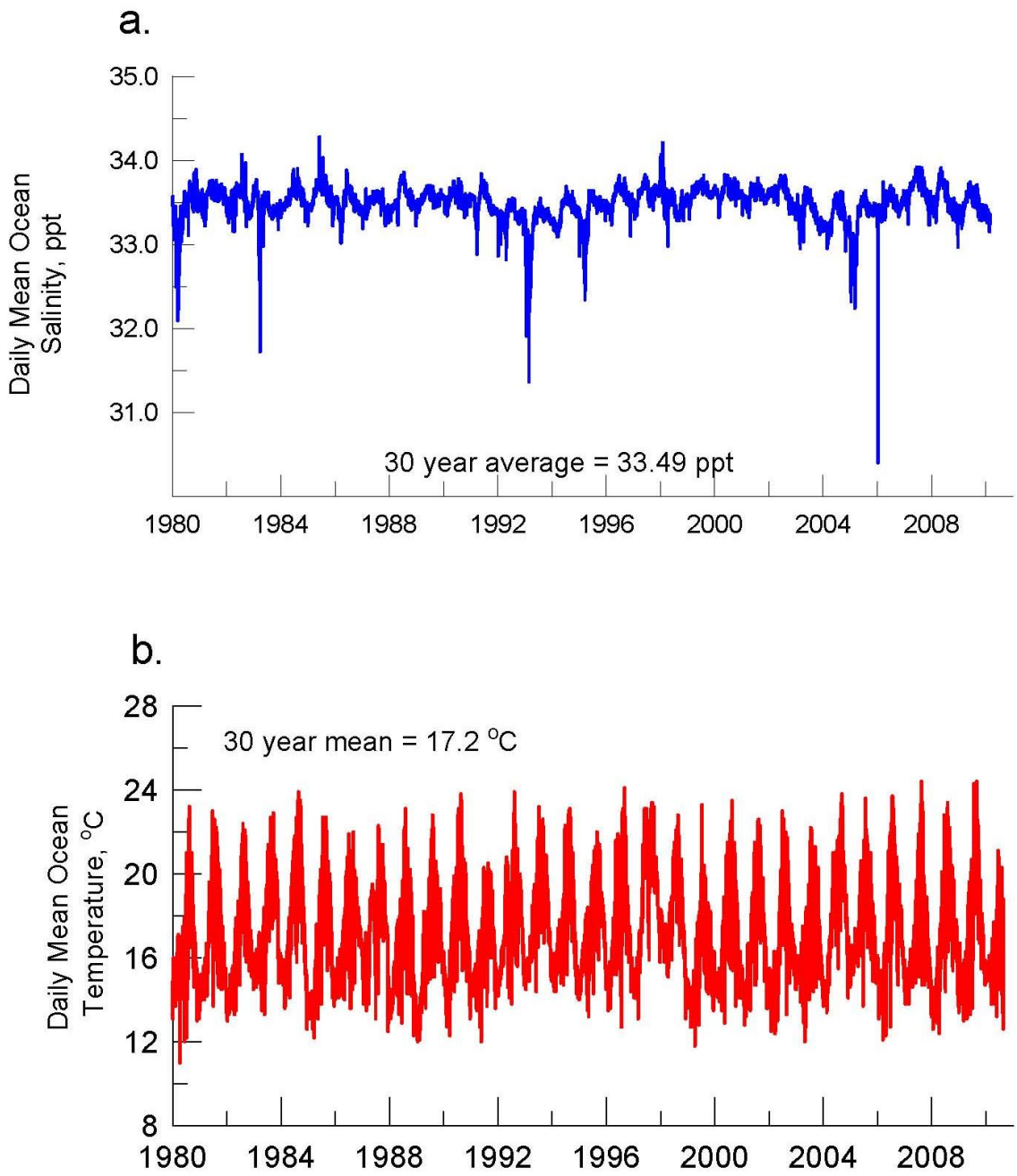

Figure 5: Daily mean ocean bottom salinity (a) and daily mean ocean bottom temperature (b) at the Carlsbad Desalination Project; from CDIP (2012), SIO, (2010), CalCOFI (2014) and NPDES/ CA0107417monitoring reports by MBC (2001-2015).

were throughput to dilution models. A pronounced seasonal variation in these temperatures is quite evident with the maximum recorded daily mean temperature reaching 25.4 ºC on the sea surface and 24.4 ºC on the seafloor during the summer of the 1993 El Niño; and the minimum falling to 9.9 ºC on the sea surface and 11.0 ºC on the seafloor during the winter of the 1999-2000 La Niña. The mean temperature was found to be 17.7 ºC on the sea surface and 17.2 ºC on the seafloor. On a percentage basis, the natural variability of the temperature of coastal waters of SJCOO is significantly greater than that of salinity, where temperature variability is on the order of $\triangle T = 86\%$ vs salinity variability of $\triangle S = 10\%$.

4.4) Temperature/Salinity Depth Profile. Under the terms within Appendix I of the *California Ocean Plan* the solution for the ZID boundary requires model input defined as, "*the trapping level when considering worst-case scenarios*". Trapping levels result from the vertical stratification of the receiving waters as a consequence of the temperature/salinity depth profile. A computer search of the temperature and salinity records in Figures 4 and 5, finds the worst-case scenario occurs in the historic record for the temperature/salinity profiles during 17 September 2008. These profiles are plotted in Figure 7. While the salinity profile is fairly uniform with depth of water, (with an average salinity of 33.47 ppt), the temperature is found to gradually decline with water depth, varying between 19.9 ^{0} C on the surface to 13.4^0 C at the seafloor. Normally there is a very abrupt change in water temperature between the warm surface mixed layer and the cold bottom water; and this abrupt change is referred to as the thermocline. The thermocline interface produces the trapping layer, where the partially diluted discharge plume no longer has sufficient momentum or buoyancy to penetrate the thermocline, and instead spreads out horizontally along the thermocline interface, resulting in a trapping level beneath the sea surface. The temperature profile in Figure 7 shows a weak thermocline and trapping level beginning at a depth of -7 to -8 m MSL. However, the temperature profile varies so gradually that the trapping level is very weak. Consequently, the brine discharge from the CDP will not be greatly retarding in subsiding through the thermocline interface and reaching the sea floor in receiving waters greater than -7 m depth.

The September 2008 salinity temperature profile was also used to define worst case scenario for the recently renewed discharge permit for the nearby San Juan Creek Ocean Outfall (NPDES NO. CA0107417 ORDER NO. R9-2012-0012), as detailed in Appendix-H of RWQCB (2014). Both the CDP and the San Juan Creek Ocean Outfall reside in the same littoral cell (the Oceanside Littoral Cell), and therefore consistency in using the same temperature/salinity depth profile to define worst-case is sensible.

33 year averages of salinity by month:

Jan = 33.44 ppt	May = 33.61 ppt	Sep = 33.54 ppt
Feb = 33.40 ppt	Jun = 33.66 ppt	Oct = 33.52 ppt
Mar = 33.35 ppt	Jul = 33.65 ppt	Nov = 33.46 ppt
Apr = 33.48 ppt	Aug = 33.61 ppt	Dec = 33.46 ppt

20 year averages of salinity by month:

Jan = 33.45 ppt	May = 33.59 ppt	Sep = 33.54 ppt
Feb = 33.40 ppt	Jun = 33.65 ppt	Oct = 33.53 ppt
Mar = 33.32 ppt	Jul = 33.64 ppt	Nov = 33.48 ppt
Apr = 33.45 ppt	Aug = 33.60 ppt	Dec = 33.48 ppt

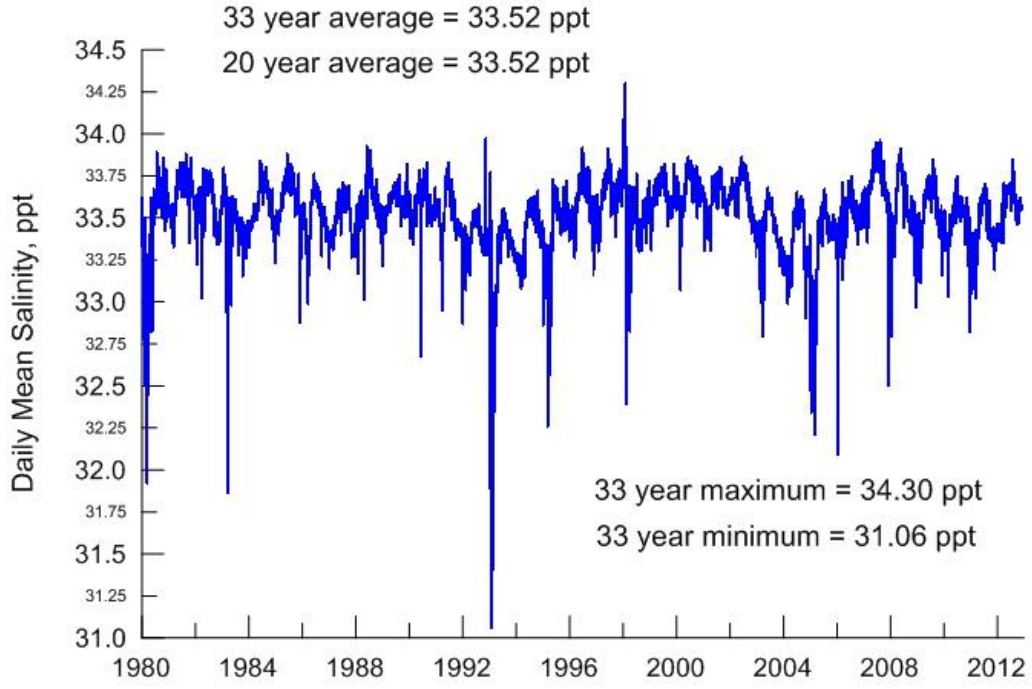

Figure 6. Natural background (ocean) salinity for dilution of discharge from the Carlsbad Desalination Plant. Period of record, 1980 to 2013 with 12,055 verified daily measurements. Data from SIO, 2013, "SIO shore station, Scripps Pier," http://www-mlrg.ucsd.edu/shoresta/mnSIOMain/siomain.htm

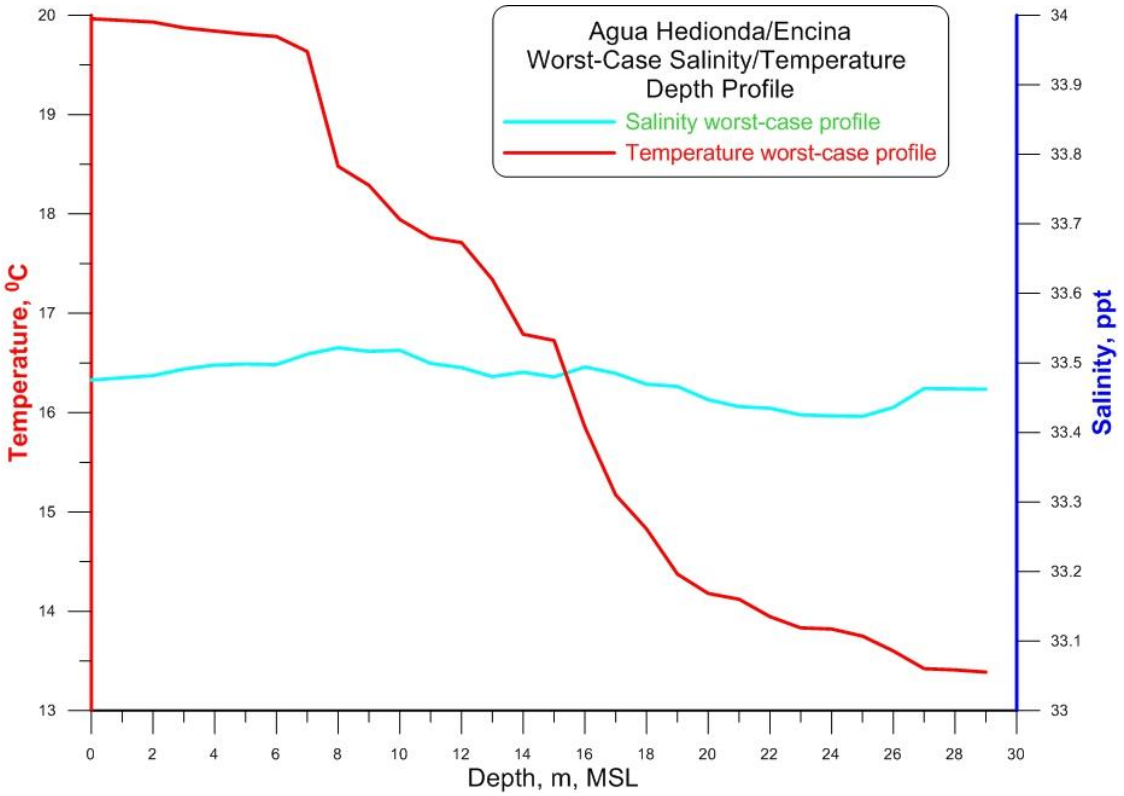

Figure 7: Worst-case temperature/salinity profile. Profiles based on 17 September 2008 upwelling and discharge conditions.

4.6) Mannings Roughness Coefficient for the Discharge Channel: The initial turbulent kinetic energy and the size of the large turbulent eddies that control the rate of initial dilution of discharge from an open channel (like that used by the CDP) are determined by the slope and roughness of the discharge channel,. These slope and roughness factors are parameterized in the nearfield dilution model by the *Manning Roughness Coefficient*, (Baumgartner, et al., 1994).

The discharge channel is a 120 ft. wide engineered trapezoidal channel bonded by a pair of rubble mound jetties with a rock rubble channel bottom (Figure 1). The north discharge jetty measures 327 ft in length from Carlsbad Blvd., while the south discharge jetty measures 376 ft in length from Carlsbad Blvd. The jetties are constructed of 7 – 10 ton quarry stone while the channel bottom is constructed of 1 ton stone quarried from the Santa Margarita River bed. The slope of the channel bottom is nominally 3% and the channel depth is -4 ft MLLW. No significant vegetation grows on the channel bottom or sidewalls. Based on standard engineering practice (per Table 1), these dimensions, slopes and materials, determine that the appropriate *base roughness coefficient* is $n_1 = 0.04$; the cross section modifier is $n_2 = 0.005$; the slope modifier is $n_3 = 0.015$ and the vegetation modifier $n_4 = 0.0$. Thus the the *Manning Roughness Coefficient* used to initialize the CORMIX 5.0 and *COSMOS/ FLowWorks* models was $\boldsymbol{n = n1 + n2 + n3 + n4 = 0.06}$

Table 1: Manning Roughness Coefficient (from Sargent, 1979)
n = n1 + n2 + n3 + n4

The Base Roughness Coefficient, n_1

- Character of Channel.....Basic ***n*** value, n_1
- Channels in earth.....0.02
- Channels cut into rock.....0.025
- Channels in fine gravel.....0.024
- Channels in coarse gravel.....0.028
- Channels engineered of rock rubble 0.040

Cross Section Modifier, n_2

- Minor (dredged or engineered channels; slightly eroded or scoured side slopes of canals).....0.005
- Moderate (fair to poor dredged channels; moderately sloughed or eroded canal side slopes).....0.010
- Severe (Badly sloughed banks of natural streams; badly eroded or sloughed sides of canals or drainage channels; unshaped, jagged and irregular surfaces of channels excavated in rock.....0.020

Slope Modifier, n_3

- Minor slopes (1-3%).....0.010-0.015
- Appreciable slopes (4-7%).....0.020-0.030
- Severe slopes (8-15%).....0.040-0.060

Vegetation Modifier, n_4

- Low.....0.005-0.010
- Medium.....0.010-0.020
- High.....0.020-0.050
- Very High.....0.050-0.100

4.7) Brine Effluent Discharge Temperature: The Carlsbad Desalination Project (CDP) begin discharging brine effluent on 1 November 2015. Appendix-1 lists intake and discharge temperatures from the CDP during the operational period from 1 November 2015 to 25 January 2016; and Appendix-2 lists intake and discharge temperatures during the operational period from 25 January to 1 April 2016. The results show an average temperature difference between intake and discharge temperatures during the first 3 operating months of $\triangle T = -0.7\ ^0F = -0.39\ ^0C$; increasing slightly to $\triangle T = +2.74\ ^0F = +1.96\ ^0C$ during the following two operating months. Therefore the CORMIX 5.0 and *COSMOS/ FLowWorks* models were initialized in two separate runs for effluent discharge streams having $\triangle T = 0\ ^0C$; and $\triangle T = +2\ ^0C$. The model runs using $\triangle T = 0\ ^0C$ give a slightly lower initial dilution because the mass diffusivity of NaCl in water (a proxy for sea salts) increases moderately with increasing temperature.

4.8) Waves, Currents, Tides and Winds: Per directives from the staff of the Regional Water Quality Control Board, San Diego Region, no excitation of receiving water motion from waves, currents, tides or winds were input to either the CORMIX 5.0 and *COSMOS/ FLowWorks* models. Ocean water levels were set at a constant elevation of 0 m MSL. We refer to this set of boundary conditions as the Quiescent Ocean Dilution condition.

5) Results for Quiescent Ocean Dilution of CDP discharge

The CDP desalination operating scenario was based on a combined intake flow rate of 299 mgd, with 238 mgd being discharged into the ocean discharge channel at a salinity of 42 ppt after blending 178 mgd of flow augmentation with the raw brin from the desalination plant. No power generation is assumed to occur within the Encina Power Station and the Delta-T of the pre-diluted brine relative to ocean water temperature is assumed to be $\triangle T = 0\ ^0C$ and $\triangle T = +2\ ^0C$ in two separate sets of model runs. The CORMIX 5.0 and *COSMOS/ FLowWorks* models were run out until the salinity distribution between two adjacent computational steps was less than 1%. At this point dilution was considered to have reached a steady state distribution. Initial dilution was considered to be complete along the loci of points in the receiving water where the dilution factor ceases to change with increasing distance from the point of discharge (gradient of Dm is less than 1%), thereby defining the outer limit of the ZID.

Figure 8 gives the bottom salinity distribution after 1,024 computational time steps for the 60 mgd upgrade of the Carlsbad Desalination Project discharging with a $\triangle T = 0\ ^0C$ into a quiescent ocean. The dispersion plot for $\triangle T = +2\ ^0C$ was indistinguishable from that in Figure 8 on the 6 km x 6 km scale of the plot; although Figure 8 does represent worst-case initial dilution because the mass diffusivity of NaCl in water (a proxy for sea salts) increases moderately with increasing temperature. Because the brine is negatively buoyant (heavier than ambient receiving water), the salinity field has been mapped over the seabed surface to represent worst-case distribution, as contoured in parts per thousand (ppt) according to the color bar scale at the figure. The regulatory brine mixing zone (BMZ) with 200m radius is shown in red. The old ZID semi-circle for thermal discharges of the Encina Power Station also shown in red with a 1000 ft. radius from end of discharge jetties. The ZID radius defined by the maximum dispersion distance of initial dilution of brine (from equations 1 – 5) is shown as white dashed semi-

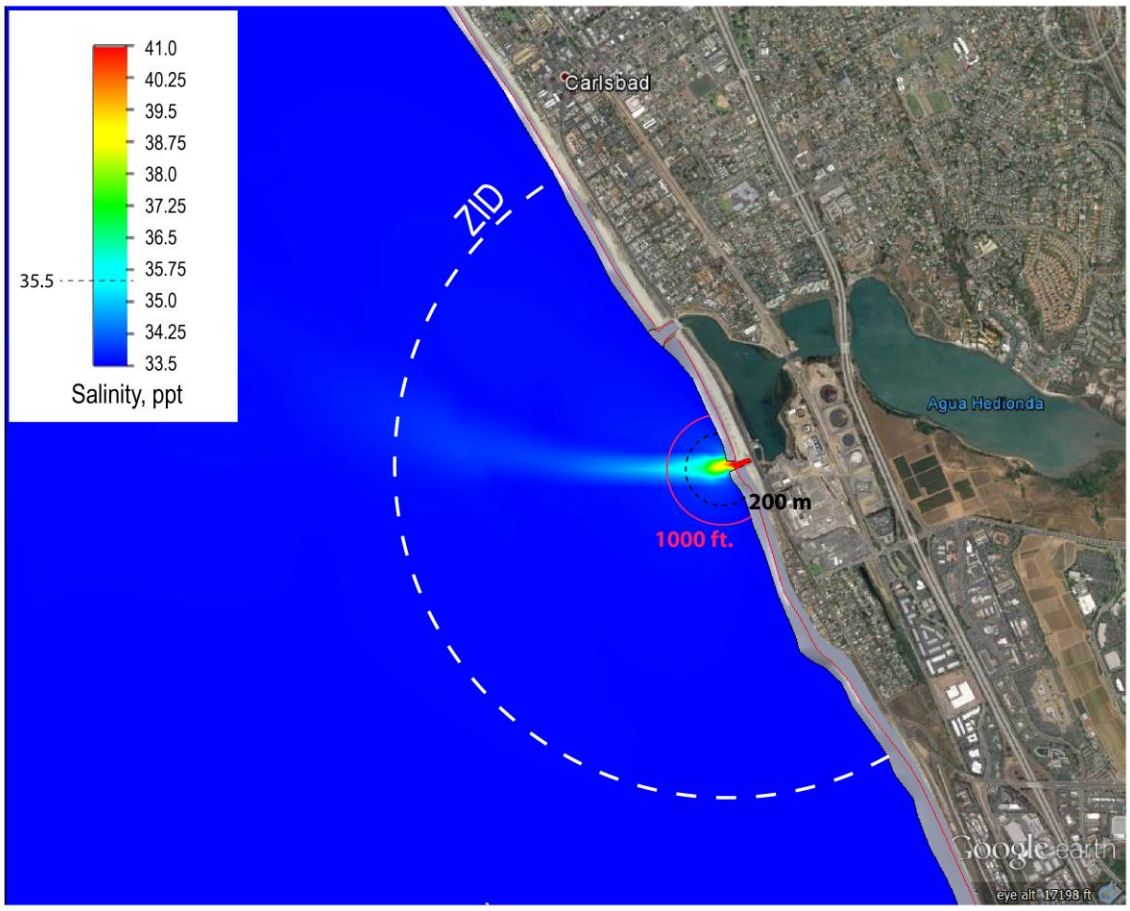

Figure 8: Bottom salinity distribution after 1,024 computational time steps for the 60 mgd upgrade of the Carlsbad Desalination Project discharging into a quiescent ocean. Total intake flow rate is 299 mgd, of which 178 mgd is flow augmentation for in-plant dilution. Product water production = 60 mgd. Total discharge = 238 mgd at 42 ppt with $\triangle T = 0\ ^{0}C$. Salinity contoured in ppt with ambient ocean salinity = 33.52 ppt. BMZ with 200m radius shown in red. ZID circle for the thermal discharge of the Encina Power Station shown in red at 1000 ft. radius from end of discharge jetties. ZID radius for brine CDP discharge from Equations (1) – (5) shown as white dashed semi-circle.

circle. There is an apparent offshore bias to the spreading of the salinity plume due to the unrestricted tendency for the denser brine to move down-slope as a gravity flow in these still water simulations following the offshore sloping bottom gradients (see Figures 2 & 3). The brine is free to move down-slope in still water, propelling itself as a gravity flow by exchanging potential energy in elevation for kinetic energy. As the brine continues down-slope it entrains a portion of the surrounding water mass, (as shown in Figures 9 and 10), diluting itself until its density is reduced to that of the surrounding water mass, when $\rho_s \rightarrow \rho$ (cf. equation 2). This occurs when the brine plume travels far enough down-slope to push across the trapping level at the thermocline (cf Figure 7) and run into colder bottom water, i.e at the point where the thermocline in the receiving water intersects the shore rise bottom profile (black offshore contour line in Figures 3 and 9 and 10). This down-slope dispersion of the hyper-salinity discharge plume is also evident in Figure 11 in a cross-shore section of the brine plume along a shoreline-normal transect following the axis of the discharge channel. As the highest salinity in the inshore portions of the plume are clearly near the bottom, as the brine plume wedges under the warm surface waters near shore (within 1,000 ft of the discharge jetties). Beyond 1000 ft from the discharge, the discharge plume meanders out of the shoreline-normal plane of Figure 11, and its signature disappears.

Comparing the offshore plume meanders in Figure 8 with Figure 3, it appears as though the dense brine plume is following bottom depressions in the micro-bathymetry formed by a series of offshore sand-waves. These bottom depressions are skewed away from the shoreline-normal alignment, diverging towards the west and causing the trajectory of the brine plume to bend in that general direction as it follows the local bottom gradients. As the brine plume follows the troughs in the bathymetric sand waves, it creates a massive system of entrainment streams and eddies as shown in Figures 9 and 10 that also exhibit this same northerly bias away from shoreline-normal alignment. This is in direct contrast to the general behavior of the brine plumes modeled in the antecedent study (Jenkins and Wasyl, 2015), where the brine plumes consistently exhibit a southerly displacement due a prevailing southerly drift from tidal currents and wave-induced longshore currents. (It should be remembered that the bathymetric depressions and troughs in Figure 3 that control the brine plume trajectory under quiescent ocean conditions are themselves ephemeral, dynamic features that could change seasonally or over longer time periods). The large-scale entrainment flow patterns and eddies shown in the quiescent ocean simulation in Figures 9 and 10 would never exist in Nature, as these organized flow features would be sheared and broken up by shoaling waves and coastal boundary layer currents.

In Figures 8 - 10, the brine plume becomes stationary at distance of 1,851 m from the ends of the discharge jetties for both the $\Delta T = 0\ ^0C$ and $\Delta T = +2\ ^0C$ outcomes. At this point, the change in dilution factor D_m with distance offshore becomes less than 1%. The Ocean Plan defines the ZID as the zone in which the process of initial dilution is completed; and since dilution ceases to increase beyond 1851 m from the point of discharge, this distance marks the seaward limit of the ZID. A white, dashed semi-circle with 1,851 m radius has been drawn around the ends of the discharge jetties in Figures 8 - 10 to denote the potential loci of points of a ZID boundary under all possible bathymetric conditions. In the Ocean Plan the concept of when initial dilution is complete is also associated with when the momentum induced velocity of the discharge ceases to produce

significant mixing of the waste. The heavy brine effluent initially has two components of momentum: 1) momentum in the velocity field (mass x velocity), and 2) momentum in the force field (force x time, or *impulsive momentum*); where the force field comes from gravity as a consequence of the negative buoyancy of the brine. As the brine begins to flow offshore and down the slopes of the nearshore bathymetry, momentum in the gravitational force field flows (*fluxes*) into the velocity field, and the brine accelerates under the force of gravity due to its negative buoyancy. Some of the gravitational acceleration is transferred to stresses of bottom friction, but the remaining momentum of the discharge stream is restructured as a system of entrainment streams and eddies, all of which derive their momentum and velocity from the initial discharge stream. The entrainment streams are *return flows* of receiving water that were displaced by the offshore-directed push (*momentum flux*) of the discharge stream, and transport receiving water into the ZID from offshore and along-shore sources which eventually merge with the discharge stream to produce dilution. Eddies are produced by shear stresses between the discharge stream and the receiving water which transfer momentum of the discharge stream into eddy momentum (*vorticity*), producing *irreversible turbulent mixing*. The dilution action of the entrainment streams and eddies dilutes the both the waste (brine) as well as the momentum contained in the discharge, until at some point offshore, the discharge becomes neutrally buoyant and the momentum of the residual velocity field is so diluted that turbulent mixing ceases. That point marks the edge of the ZID, and can be inferred from the velocity field as the zone beyond which organized eddy motion ceases.

Obviously the ZID for brine discharge is considerably larger than the historic 1000ft radius ZID that the Encina Power Station has operated under with prior NPDES permits. However, first it must be noted that thermal effluent is buoyant and disperses over a flat ocean surface (or trapping layer) which produces no slope along which the gravitational force field can accelerate the discharge stream. Second, the efficacy of the large brine ZID is apparent in the large scale eddies of Figures 9 and 10 which extend great distances offshore. Note that there is little difference in the entrainment streams between the $\triangle T = 0\ ^0C$ case in Figure 9 and the $\triangle T = +2\ ^0C$ case in Figure 10; and only minor differences in the eddy structures near the ZID boundary. These large-scale entrainment streams and eddies that are present inside and close to the ZID boundary indicate that dilution is still occurring very far offshore. Furthermore, the brine plume in Figure 8 does not fully extinguish until reaching the ZID boundary; where light blue traces of hyper-salinity do not disappear until reaching the ZID, whence initial dilution is completed.

Because the discharge plume meanders to some degree and does not follow a particular shoreline normal plane, the CORMIX 5.0 and *COSMOS/ FLowWorks* matched solutions of still water dilution were evaluated along a series of radials projected at 1^0 increments outward from the end of the discharge jetties, to find the worst case relationship between dilution and distance. The results are plotted in Figure 12 for $\triangle T = 0\ ^0C$ and in Figure 13 for $\triangle T = +2\ ^0C$; where the discharge salinity maximum is plotted in red according to the right hand axis as a function of distance along worst case radial; and dilution factor, D_m, is plotted in blue against the left hand axis. A tabular summary of discharge salinity and dilution factor values is found in Table 2 for intermediate distances along worst case radials from the point of discharge. We find that the $2\ ^0C$ variance in ΔT has little effect on the results, and that the salinity maxima decline to 2 ppt over natural

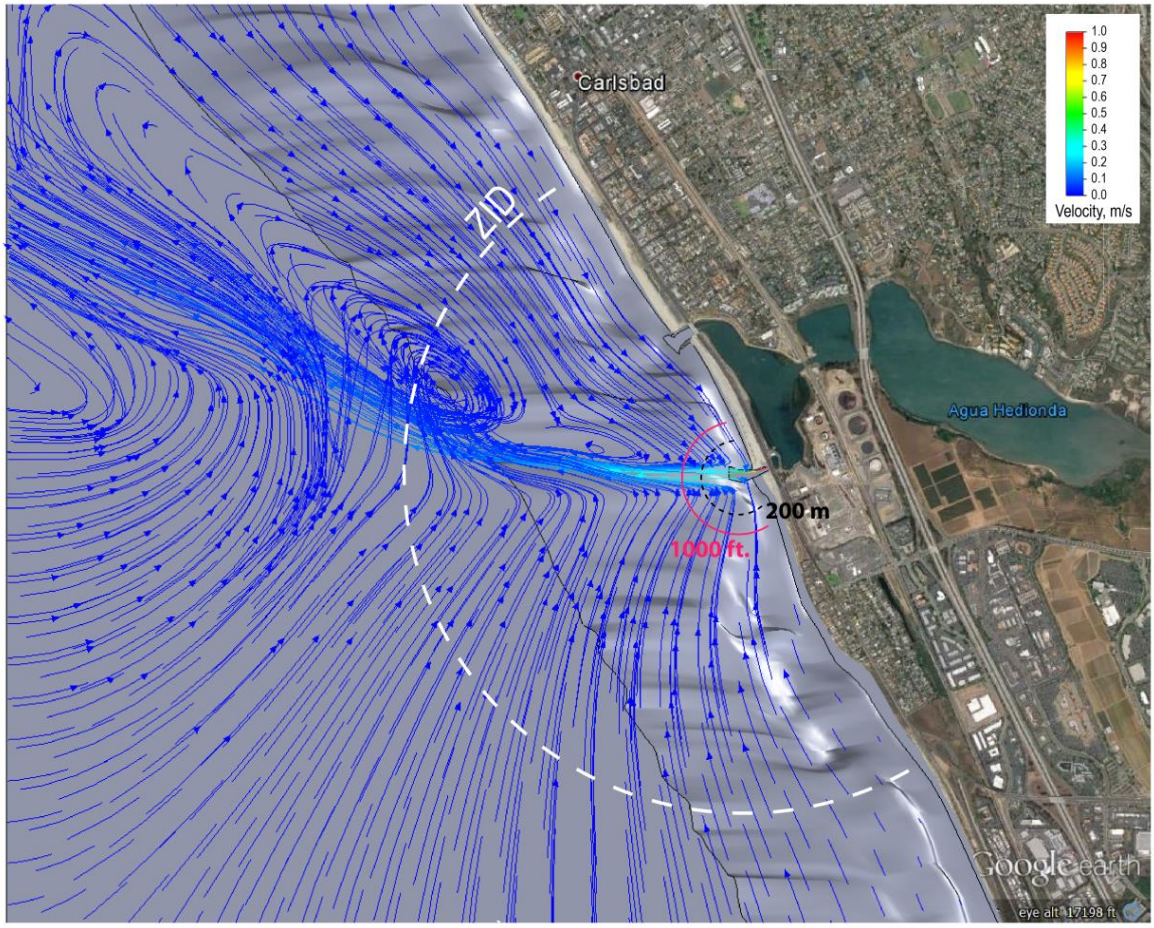

Figure 9: Streamline pattern of brine discharge jet and entrainment flow after 1,024 computational time steps for the 60 mgd upgrade of the Carlsbad Desalination Project discharging into a quiescent ocean. Total intake flow rate is 299 mgd, of which 178 mgd is flow augmentation for in-plant dilution. Product water production = 60 mgd. Total discharge = 238 mgd at 42 ppt with $\Delta T = 0\ ^0C$. Salinity contoured in ppt with ambient ocean salinity = 33.52 ppt. BMZ with 200m radius shown in red. ZID circle for the thermal discharge of the Encina Power Station shown in red at 1000 ft. radius from end of discharge jetties. ZID radius for brine CDP discharge from Equations (1) – (5) shown as white dashed semi-circle. Intersection of trapping level with the seabed shown as black offshore contour.

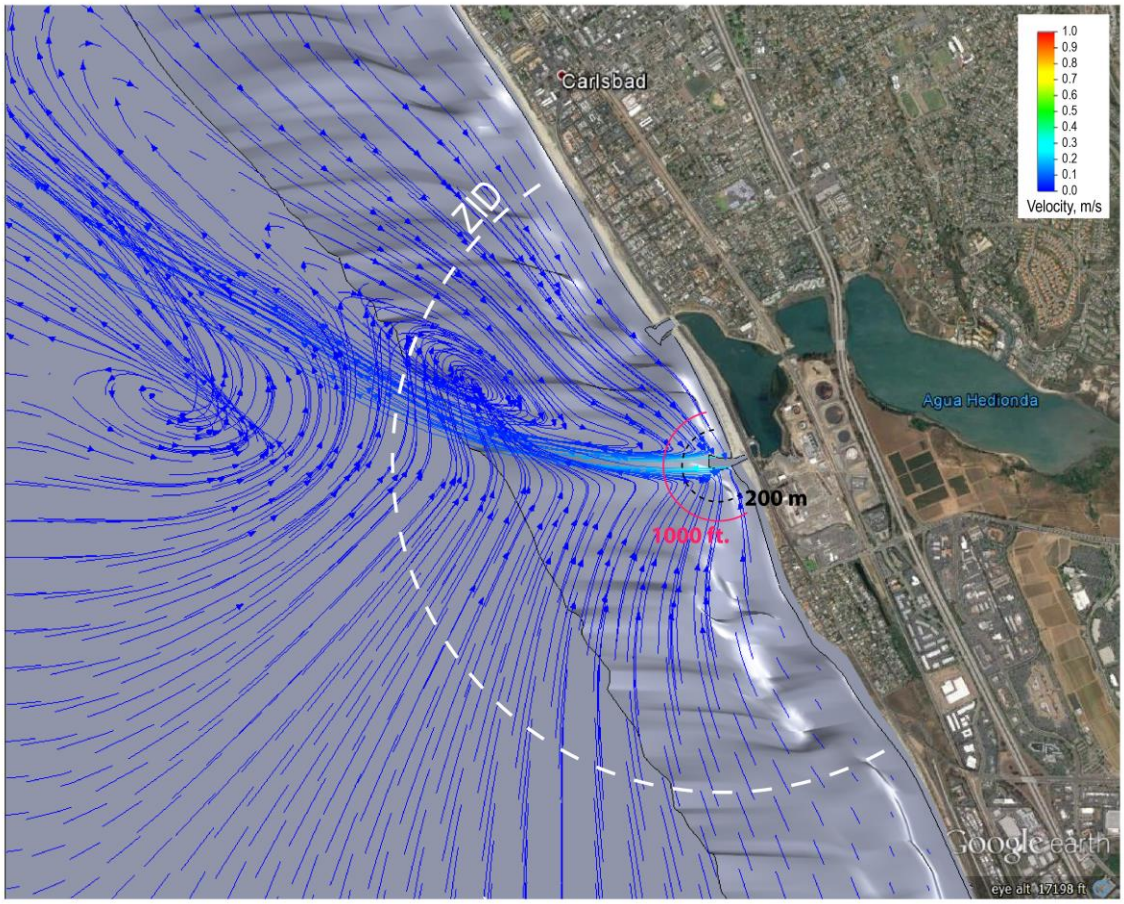

Figure 10: Streamline pattern of brine discharge jet and entrainment flow after 1,024 computational time steps for the 60 mgd upgrade of the Carlsbad Desalination Project discharging into a quiescent ocean. Total intake flow rate is 299 mgd, of which 178 mgd is flow augmentation for in-plant dilution. Product water production = 60 mgd. Total discharge = 238 mgd at 42 ppt with $\Delta T = 2\ ^{0}C$. Salinity contoured in ppt with ambient ocean salinity = 33.52 ppt. BMZ with 200m radius shown in red. ZID circle for the thermal discharge of the Encina Power Station shown in red at 1000 ft. radius from end of discharge jetties. ZID radius for brine CDP discharge from Equations (1) – (5) shown as white dashed semi-circle. Intersection of trapping level with the seabed shown as black offshore contour.

background at a distance of 196 m from the point of discharge, where Dm = 3.25. At the 200 m BMZ boundary, the maxima in discharge salinity is 35.47 ppt, thereby satisfying the brine amendment of the California Ocean Plan, (Appendix-A of SWRCB 2015). The corresponding dilution factor is $D_m = 3.31$ at the BMZ 200 m boundary, where Dm is calculated based on 42 parts per thousand (ppt) effluent concentration in the discharge pond (point M-002). This result is within the statistical spread of dilution results in the antecedent study when corrected for partially diluted brine as it leaves the discharge pond, (cf. Figure 18 in Jenkins and Wasyl, 2015). At the historic 1,000 ft radius ZID written in NPDES permits for Encina Power Station, maximum brine salinity is diluted to 34.9 ppt with a corresponding dilution $D_m = 5.07$ for a $\triangle T = 0\ ^0C$; and $D_m = 5.08$ for a $\triangle T = +2\ ^0C$. At the CDP brine ZID, where brine dilution achieves a steady end state, initial dilution reaches a robust $D_m = 52.1$ to 1 for a $\triangle T = 0\ ^0C$ (Figure 12); increasing slightly to $D_m = 55.0$ to 1 for a $\triangle T = +2\ ^0C$, (Figure 13).

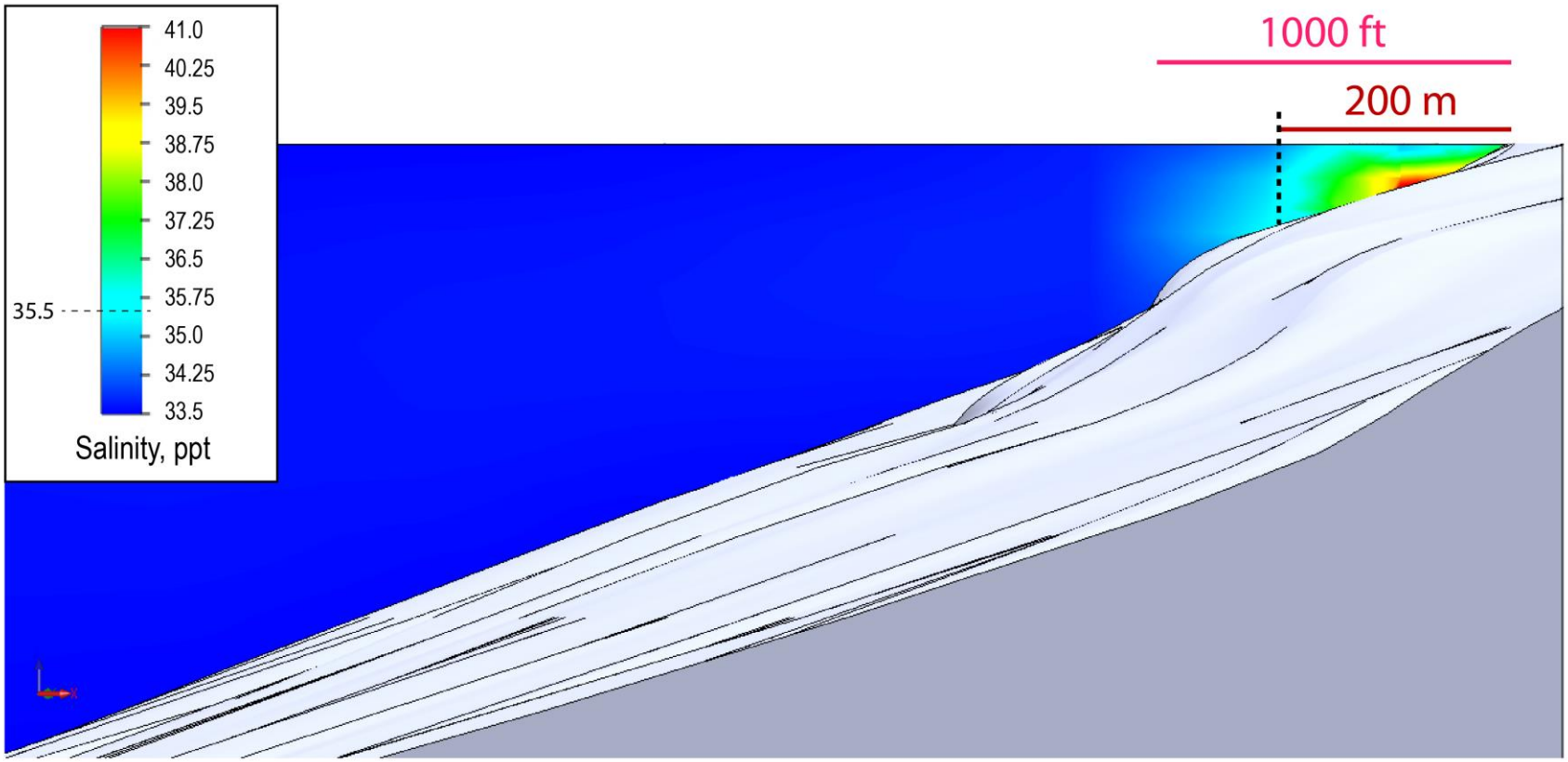

Figure 11: Cross-shore section of the brine plume along a shoreline-normal transect along the axis of the discharge channel. Total intake flow rate is 299 mgd, of which 178 mgd is flow augmentation for in-plant dilution. Product water production = 60 mgd. Total discharge = 238 mgd at 42 ppt with $\triangle T = 0\ ^0C$. Salinity contoured in ppt with ambient ocean salinity = 33.52 ppt. BMZ with 200m radius shown in red. ZID for thermal discharge of the Encina Power Station shown in red at 1000 ft. radius. Vertical exaggeration is 19 to 1.

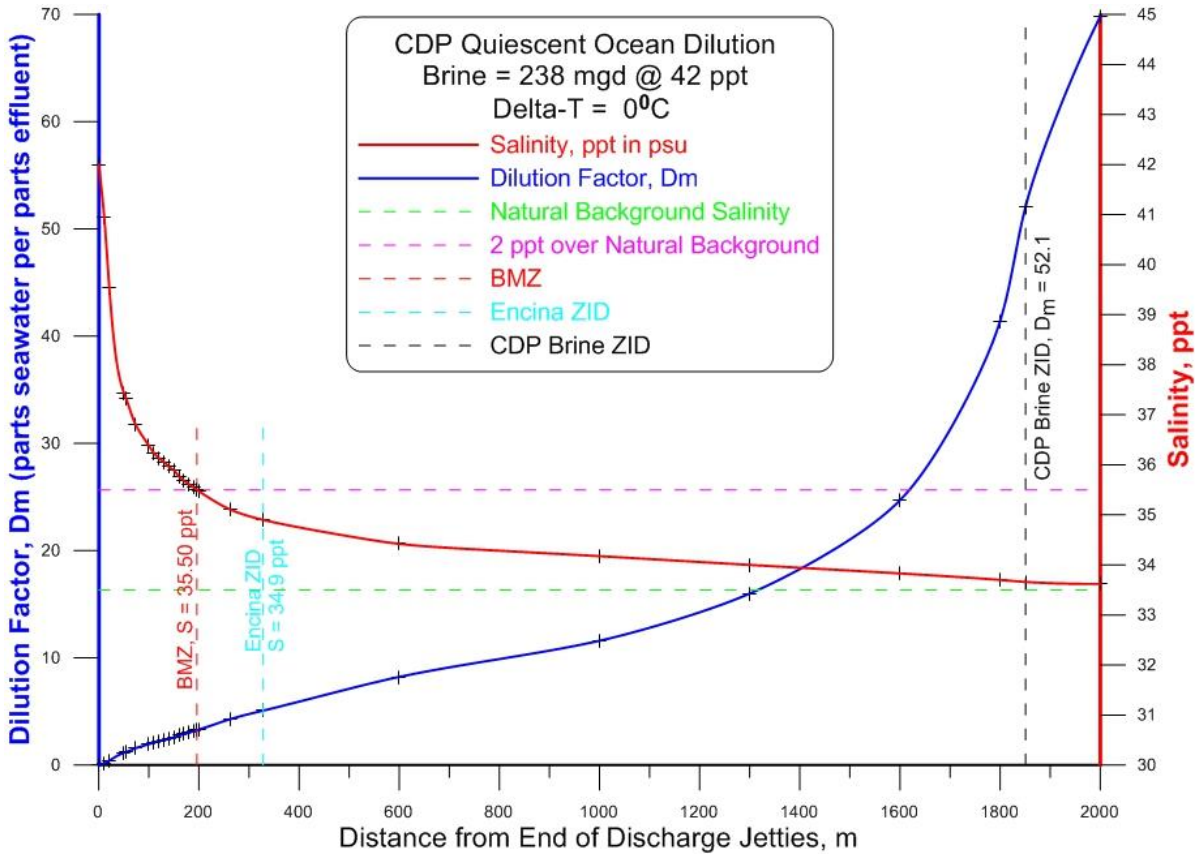

Figure 12: CORMIX 5.0 and *COSMOS/ FLowWorks* matched solution of still water dilution of CDP brine discharge = 238 mgd at 42 ppt, with $\triangle T = 0\ ^0C$. Discharge salinity maximum (red, right hand axis) as a function of distance along worst case radial from end of discharge jetties. Dilution factor, Dm, (blue, left hand axis) as a function of distance along worst case radial from end of discharge jetties. Dm based on 42 parts per thousand (ppt) effluent concentration at M-002.

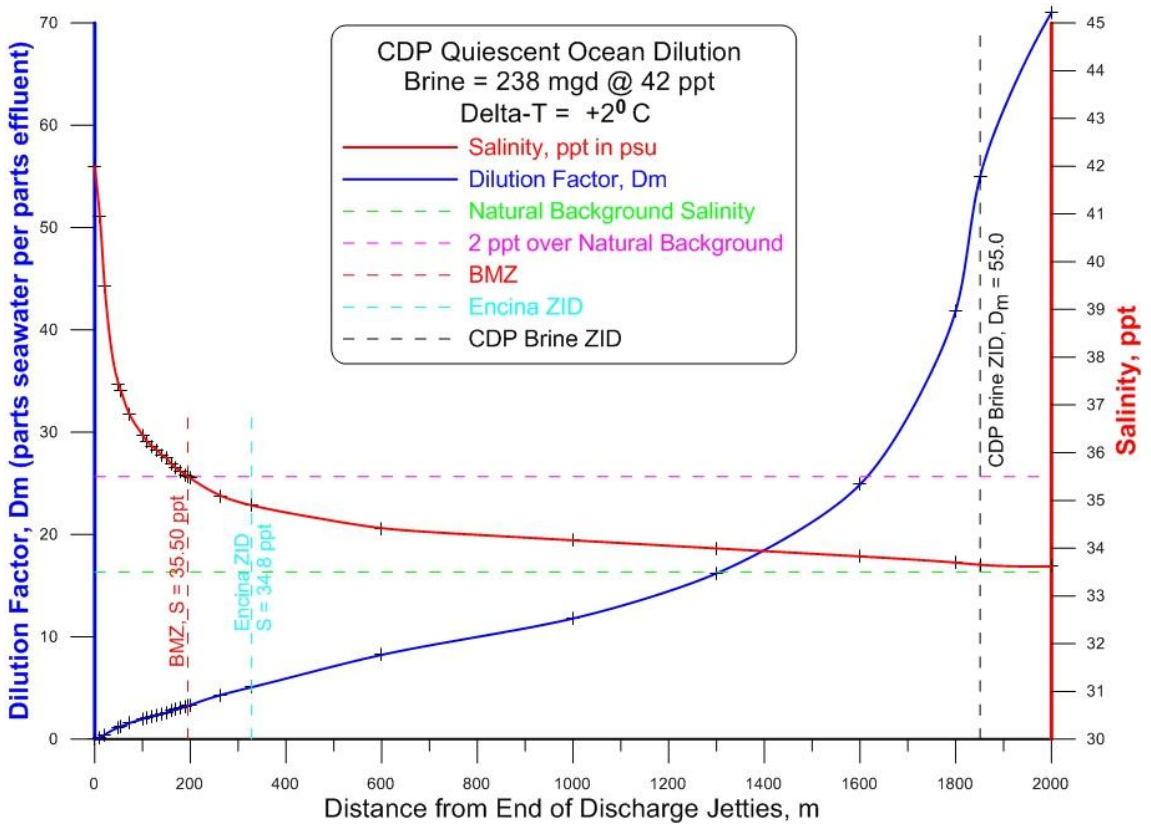

Figure 13: CORMIX 5.0 and *COSMOS/ FLowWorks* matched solution of still water dilution of CDP brine discharge = 238 mgd at 42 ppt, with $\triangle T = +2\ ^{0}C$. Discharge salinity maximum (red, right hand axis) as a function of distance along worst case radial from end of discharge jetties. Dilution factor, Dm, (blue, left hand axis) as a function of distance along worst case radial from end of discharge jetties. Dm based on 42 parts per thousand (ppt) effluent concentration at M-002.

Table 2: Summary of minimum monthly dilution (Dm) as a function of distance from the point of discharge into the receiving water.

Distance from Discharge, (m)	Maximum Salinity of Discharge for $\Delta T = 0^0$ C, (ppt)	Maximum Salinity of Discharge for $\Delta T = +2^0$ C, (ppt)	*Dilution Factor, Dm, for $\Delta T = 0^0$ C	*Dilution Factor, Dm, for $\Delta T = +2^0$ C
0.00	42.000	42.000	0	0
10.78	40.956	40.956	0.14	0.14
21.07	39.528	39.485	0.41	0.42
50.19	37.435	37.435	1.16	1.16
54.90	37.311	37.294	1.23	1.24
73.17	36.807	36.794	1.57	1.58
100.0	36.381	36.371	1.95	1.96
110.0	36.233	36.232	2.11	2.11
120.0	36.131	36.130	2.23	2.23
130.0	36.060	36.059	2.32	2.32
140.0	35.956	35.949	2.46	2.47
150.0	35.901	35.894	2.54	2.55
160.0	35.760	35.754	2.76	2.77
170.0	35.685	35.679	2.89	2.90
180.0	35.614	35.609	3.02	3.03
190.0	35.543	35.538	3.16	3.17
196.0	35.502	35.495	3.25	3.26
200.0	35.472	35.467	3.31	3.32
264.0	35.100	35.097	4.31	4.32
328.1	34.900	34.898	5.07	5.08
600.0	34.420	34.419	8.23	8.24
1000	34.174	34.164	11.6	11.8
1300	34.011	33.994	16.0	16.2
1600	33.830	33.828	24.7	24.9
1800	33.700	33.698	41.4	41.9
1851	33.660	33.651	52.1	55.0
2000	33.621	33.618	69.8	71

*Based on 42 parts per thousand (ppt) effluent concentration at M-002; where:

$$D_m = \frac{S_b(M002) - S_b(x)}{S_b(x) - S_0}$$

Here: $S_b(M002)$ = 42 ppt and is the effluent discharge salinity in the discharge pond at, $x = M002$; $S_b(x)$ is the effluent salinity in the discharge plume at a distance x from the point of discharge (end of the discharge jetties); and S_0 is the natural background salinity in the receiving water.

6) Conclusions:

A set of coupled high resolution dilution models were constructed and run to resolve initial dilution of concentrated seawater and trace pollutants at the boundaries of the zone of initial dilution (ZID) under stand-alone operations of the Carlsbad Desalination Project (CDP). Peer reviewed, published and USEPA certified hydrodynamic models were employed to resolve initial dilution and discharge plume trajectories under standard NPDES dilution modeling protocols (as defined in the California Ocean Plan); according to which "*Initial Dilution will be considered the process which results in the rapid and irreversible turbulent mixing of wastewater with ocean water around the point of discharge".* As such the models do not consider any additional mixing due to the action of ocean currents, waves, tides or wind. The models were initialized for quiescent ocean receiving waters at mean sea level bounded by the existing beach and offshore bathymetry surrounding the discharge channel for the Carlsbad Desalination Project. The discharge channel was initialized in the models according to as-built drawings, thereby establishing the appropriate Manning's roughness coefficient that corresponds to the size of stone used in construction of the discharge jetties and discharge channel bottom. The models evaluate initial dilution for effluent discharge streams of 238 mgd with a salinity of 42 ppt in the discharge pond east of Carlsbad Blvd., prior to discharge into the shorezone through the discharge channel. Effluent discharge streams were assumed to be within a couple of degrees of ambient ocean temperature ($\triangle T = 0$ to $+ 2\ ^0C$) based on temperature monitoring data after 5 months of operations of the CDP. Ocean receiving waters were initialized with the monthly mean temperature and salinity profiles that result in a minimum initial dilution (minimum month). The minimum month was determined to be September 2008, the same minimum month scenario that was used for the recently renewed discharge permit for the nearby San Juan Creek Ocean Outfall (NPDES NO. CA0107417 ORDER NO. R9-2012-0012). Both the CDP and the San Juan Creek Ocean Outfall reside in the same littoral cell (the Oceanside Littoral Cell), and therefore consistency in using the same temperature/salinity depth profile to define worst-case is sensible. Initial dilution was considered to be complete along the loci of points in the receiving water where the gradient in dilution factor is less than 1%. Initial dilution was considered to have reached a steady state along that loci of points when the variance in dilution factor between two adjacent computational steps became less than 1%.

The matched CORMIX 5.0 and *COSMOS/ FLowWorks* model solutions of still water dilution of CDP brine discharge show that it flows downslope and offshore as a gravity flow, by exchanging potential energy in elevation for kinetic energy and following bottom depressions in the micro-bathymetry formed by a series of offshore sand-waves. These bottom depressions are skewed away from the shoreline-normal alignment, diverging towards the west-northwest and causing the trajectory of the brine plume to bend in that general direction as it follows the local bottom gradients. As the brine plume follows the troughs in the bathymetric sand waves, it creates a massive system of entrainment streams and eddies that also exhibit this same northwesterly bias away from shoreline-normal alignment. This is in direct contrast to the general behavior

of the brine plumes modeled in the antecedent study (Jenkins and Wasyl, 2015), where the brine plumes consistently exhibit a southerly displacement due a prevailing southerly drift from tidal currents and wave-induced longshore currents. The large-scale entrainment flow patterns and eddies in the quiescent ocean simulations would never exist in Nature, as these organized flow features would be sheared and broken up by shoaling waves and coastal boundary layer currents.

The brine plume becomes stationary at distance of 1,851 m from the ends of the discharge jetties. At this point, the change in dilution factor D_m with distance offshore becomes less than 1% and dilution is considered complete, marking the seaward limit of the *zone of initial dilution* (ZID). Initial dilution at the ZID reaches a robust dilution factor of $D_m = 52.1$ to 1 for a $\triangle T = 0\ ^0C$; increasing slightly to $D_m = 55.0$ to 1 for a $\triangle T = +2\ ^0C$. These determinations of Dm are based on an effluent concentration of 42 ppt in the discharge pond (compliance point M-002). We find that the salinity maxima decline to 2 ppt over natural background at a distance of 196 m from the point of discharge, where Dm = 3.25. At the 200 m BMZ boundary, the maxima in discharge salinity is 35.47 ppt, thereby satisfying the brine amendment of the California Ocean Plan, (Appendix-A of SWRCB 2015). The corresponding dilution factor is $D_m = 3.31$ at the BMZ 200 m boundary. This result is within the statistical spread of dilution results in the antecedent study when corrected for partially diluted brine as it leaves the discharge pond, (cf. Figure 18 in Jenkins and Wasyl, 2015). At the historic 1,000 ft radius ZID written in NPDES permits for Encina Power Station, maximum brine salinity is diluted to 34.9 ppt with a corresponding dilution $D_m = 5.07$ for a $\triangle T = 0\ ^0C$; and $D_m = 5.08$ for a $\triangle T = +2\ ^0C$. The weak sensitivity of dilution a great distance to Delta-T variance is due to the fact that the mass diffusivity of NaCl in water (a proxy for sea salts) increases moderately with increasing temperature, with $\triangle T = 0\ ^0C$ representing worst-case initial dilution.

8) References:

Batchelor, G. K., 1970, *An Introduction to Fluid Mechanics,* Cambridge Univ. Press, New York., 615 pp.

Baumgartner, D. J.,, W.E. Frick, and P.J.W. Roberts, 1994, "EPA Dilution Models for Effluent Discharges", Third Addition, U.S. Environmental Protection Agency, Standards and Applied Science Division Office of Science and Technology, 199 pp.

CalCOFI, 2014, "California Cooperative Oceanic Fisheries Investigation", Southern California Coastal Ocean Observation System, SCOOS Data: http://www.calcofi.org/data/sccoos/sccoos-data.html

CDIP (2012), "Coastal data information program," *SIO Reference Series*, 01-20 and http://cdip.ucsd.edu.

EIR, 2005 "Precise Development Plan and Desalination Plant," EIR 03-05-Sch #2004041081, prepared for City of Carlsbad by Dudek and Associates, December, 2005.

Elwany, M. H. S., A. L. Lindquist, R. E. Flick, W. C. O'Reilly, J. Reitzel and W. A. Boyd, 1999, "Study of Sediment Transport Conditions in the Vicinity of Agua Hedionda Lagoon," submitted to California Coastal Commission, San Diego Gas & Electric, City of Carlsbad.

Elwany, M. H. S., R. E. Flick, M. White, and K. Goodell, 2005, "Agua Hedionda Lagoon Hydrodynamic Studies," prepared for Tenera Environmental, 39 pp. + appens.

Graham, J. B., 2004, "Marine biological considerations related to the reverse osmosis desalination project at the Applied Energy Sources, Huntington Beach Generating Station," Appendix-S in REIR, 2005,
100 pp.

Inman, D. L., M. H. S. Elwany & S. A. Jenkins, 1993, "Shoreline and bar-berm profiles on ocean beaches," *Jour. Geophys. Res.,* v. 98, n. C10, p. 18,181–18,199.

Jenkins, S. A. and J. Wasyl, 2005, "Hydrodynamic Modeling of Dispersion and Dilution of Concentrated Seawater Produced by the Ocean Desalination Project at the Encina Power Plant, Carlsbad, CA, Part II: Saline Anomalies due to Theoretical Extreme Case Hydraulic Scenarios*,"* submitted to Poseidon Resources, 97pp.

Jenkins, S. A. and J. Wasyl, 2005, "Coastal evolution model," Scripps Institution of Oceanography Tech Report No. 58, 179 pp + appendices. http://repositories.cdlib.org/sio/techreport/58/

Jenkins, S. A. and D. L. Inman, 2006, "Thermodynamic solutions for equilibrium beach profiles", *Jour. Geophys. Res.,* v.3, C02003, doi:10.1029/2005JC002899, 2006. 21pp

Jenkins, S. A., J. Paduan, P. Roberts, D. Schlenk, and J. Weis, 2012, "Management of Brine Discharges to Coastal Waters; Recommendations of a Science Advisory Panel", submitted at the request of the California Water Resources Control Board, 56 pp. + App.

Jenkins, S. A., 2013, "Technical Memorandum: Shoreline Evolution Analysis of Impacts Related to Removal of the South Beach Groin at Encina Power Station, Carlsbad," submitted to NRG Energy, 90 pp.

Jenkins, S. A. and J. Wasyl, 2015, "Hydrodynamic Dilution Analysis for the Carlsbad Desalination Project Operating at Sixty Million Gallons Per Day Production Rate", submitted to Poseidon Water, LLC 48 pp.

RWQCB, 2014, "ORDER NO. R9-2012-0012, NPDES NO. CA0107417 WASTE DISCHARGE REQUIREMENT FOR THE SOUTH ORANGE COUNTY WASTEWATER AUTHORITY, DISCHARGE TO THE PACIFIC OCEAN THROUGH THE SAN JUAN CREEK OCEAN OUTFALL, APPENDIX-H DILUTION MODEL INFORMATION" CALIFORNIA REGIONAL WATER QUALITY CONTROL BOARD SAN DIEGO REGION, 8 pp.

RWQCB, 2015, "Regional Water Quality Control Board (Regional Water Board) Order No. R9-2006-0065 (NPDES CA0109223)" 54 pp

Sargent, R J., 1979, "Variation of Mannings roughness coefficient with flow in open channels", *Jour Inst. Water Eng.*, v. 33, no. 3, p. 290 -294.

SCCWRP, 2012, Southern California Coastal Water Research Project: "Management of Brine Discharges to Coastal Waters - Recommendations of a Science Advisory Panel. Technical Report 694 to the State Water Resources Control Board, Southern California Coastal Water Research Project, Costa Mesa, CA.

SCCOOS, 2014, "Southern California Coastal Ocean Observation System", Current Data, SJCOO: http://www.sccoos.org/data/hfrnet/

SIO, 2013, "SIO shore station, Scripps Pier", http://www-mlrg.ucsd.edu/shoresta/mnSIOMain/siomain.htm

SWRCB, 2015, Amendment to the Water Quality Control Plan For Ocean Waters of California Addressing: "DESALINATION FACILITY INTAKES, BRINE DISCHARGES, AND THE INCORPORATION OF OTHER NON-SUBSTANTIVE CHANGES", cf. Appendix-A: "Ocean Plan with the May 6, 2015 Final Desalination Amendment", 1303 pp.

Star-CD, 1998 Manuals Version 3.1, *Computational Dynamics*. 1999.

Tenera, 2008, **"**Cabrillo Power I LLC, Encina Power Station 316(b) Cooling Water Intake Impingement Mortality and Entrainment Characterization Study: Effects on the Biological Resources of Agua Hedionda Lagoon and the Nearshore Ocean Environments" submitted to NRG Energy, 220 pp

USACE, 1993, "Existing State of San Diego County Coast," US Army Corps of Engineers, Los Angeles District, Tech Rpt 93-1, 335 pp.

Voorhees, J.P., B.M. Phillips, B.S. Anderson, K. Siegler, S. Katz, L. Jennings, R.S. Tjeerdema, J. Jensen, and M. de la Paz Capio-Obeso. 2013. Hypersalinity toxicity thresholds for nine California Ocean Plan toxicity test protocols. *Archives of Environmental Contamination and Toxicology* 65:665-670

Weston Solutions, (2013), "High-Salinity Sensitivity Study: Short- and Long-Term Exposure Assessments", submitted to West Basin Municipal Water District, 571 pp. http://www.waterboards.ca.gov/water_issues/programs/ocean/desalination/dos/salstudy4wbmd.

Appendix-1: Intake and Discharge Temperatures of the Carlsbad Desalination Project, 1 November 2015 to 25 January 2016

Location	Date	Time	Intake Temp ^{o}F	Discharge Temp ^{o}F	Increased Temp ^{o}F
M-001	11/1/2015	8:44	65.4	72.0	6.6
M-001	11/2/2015	9:15	72.1	68.6	-3.5
M-001	11/3/2015	12:50	70.3	68.5	-1.8
M-001	11/4/2015	9:10	67.2	66.2	-1.0
M-001	11/5/2015	14:00	72.9	68.0	-4.9
M-001	11/6/2015	7:35	64.9	68.6	3.7
M-001	11/7/2015	12:00	68.2	69.0	0.8
M-001	11/8/2015	9:45	68.2	67.8	-0.4
M-001	11/9/2015	9:50	68.7	68.4	-0.3
M-001	11/14/2015	19:30	61.1	ND	n/a
M-001	11/15/2015	15:30	68.0	65.5	-2.5
M-001	11/16/2015	16:14	64.9	63.0	-1.9
M-001	11/17/2015	12:15	64.9	61.8	-3.1
M-001	11/18/2015	10:00	67.0	65.5	-1.5
M-001	11/19/2015	11:15	65.6	68.3	2.7
M-001	11/20/2015	9:26	67.3	64.0	-3.3
M-001	11/21/2015	9:30	68.9	65.8	-3.1
M-001	11/22/2015	8:36	69.0	65.9	-3.1
M-001	11/23/2015	7:25	68.1	65.6	-2.5
M-001	11/24/2015	9:35	66.8	72.0	5.2
M-001	11/25/2015	10:25	67.7	65.8	-1.9
M-001	11/26/2015	9:10	64.9	64.6	-0.3
M-001	11/27/2015	8:15	66.4	64.4	-2.0
M-001	11/28/2015	9:55	64	63.9	-0.1
M-001	11/29/2015	9:05	65.2	63.1	-2.1
M-001	11/30/2015	8:30	65.3	62.7	-2.6
M-001	12/1/2015	10:15	69.4	69.0	-0.4
M-001	12/2/2015	7:22	66.6	68.6	2.0
M-001	12/3/2015	7:50	65.1	63.2	-1.9
M-001	12/4/2015	8:55	67.4	66.5	-0.9
M-001	12/5/2015	12:30	71.4	68.5	-2.9
M-001	12/6/2015	8:00	64.8	64.0	-0.8
M-001	12/7/2015	10:45	67.8	69.9	2.1
M-001	12/8/2015	8:50	64.0	64.4	0.4
M-001	12/9/2015	8:15	66.6	65.2	-1.4
M-001	12/10/2015	8:50	68.9	67.6	-1.3

M-001	12/11/2015	8:50	66.4	64.3	-2.1
M-001	12/12/2015	19:58	63.6	65.4	1.8
M-001	12/13/2015	15:45	66.5	63.1	-3.4
M-001	12/15/2015	16:00	68.1	ND	n/a
M-001	12/16/2015	9:35	60.9	ND	n/a
M-001	12/16/2015	9:35	60.9	ND	n/a
M-001	12/17/2015	14:05	61.4	ND	n/a
M-001	12/18/2015	8:10	61.5	ND	n/a
M-001	12/19/2015	17:20	61.3	ND	n/a
M-001	12/20/2015	9:30	62.0	ND	n/a
M-001	12/21/2015	9:15	62.6	ND	n/a
M-001	12/22/2015	8:10	62.0	62.2	0.2
M-001	12/23/2015	10:35	68.0	62.0	-6.0
M-001	12/30/2015	9:15	58.9	57.6	-1.3
M-001	1/3/2016	11:49	59.1	61.9	2.8
M-001	1/10/2016	10:35	62.3	63.3	1.0
M-001	1/19/2016	9:28	64.7	66.9	2.2
M-001	1/25/2016	9:45	63.0	63.0	0.0
Average					**-0.7**

Appendix-2: Intake and Discharge Temperatures of the Carlsbad Desalination Project, 27 January 2016 to 1 April 2016

From date	To date	Intake Temp (TIT100-008) oF Weighted Avg	RO Brine Temp. (TIT500-001/1-14) oF	deltaT RO Brine - Intake Temp. oF	deltaT RO Brine - Intake Temp. oC
1/26/2016 0:00	1/27/2016 0:00	60.47	65.45	4.98	2.77
1/27/2016 0:00	1/28/2016 0:00	62.73	67.43	4.70	2.61
1/28/2016 0:00	1/29/2016 0:00	62.25	67.16	4.91	2.73
1/29/2016 0:00	1/30/2016 0:00	62.12	67.03	4.90	2.72
1/30/2016 0:00	1/31/2016 0:00	60.53	65.56	5.03	2.80
1/31/2016 0:00	2/1/2016 0:00	60.59	65.53	4.94	2.74
2/1/2016 0:00	2/2/2016 0:00	58.42	63.44	5.02	2.79
2/2/2016 0:00	2/3/2016 0:00	59.88	64.66	4.79	2.66
2/3/2016 0:00	2/4/2016 0:00	60.43	65.21	4.78	2.66
2/4/2016 0:00	2/5/2016 0:00	61.78	66.92	5.15	2.86
2/5/2016 0:00	2/6/2016 0:00	58.60	64.02	5.42	3.01
2/6/2016 0:00	2/7/2016 0:00	58.35	63.60	5.26	2.92
2/7/2016 0:00	2/8/2016 0:00	58.48	63.12	4.64	2.58
2/8/2016 0:00	2/9/2016 0:00	60.95	65.38	4.43	2.46
2/9/2016 0:00	2/10/2016 0:00	60.97	66.32	5.35	2.97
2/10/2016 0:00	2/11/2016 0:00	59.78	65.10	5.32	2.95
2/11/2016 0:00	2/12/2016 0:00	60.22	65.45	5.23	2.90
2/12/2016 0:00	2/13/2016 0:00	60.25	65.26	5.01	2.78
2/13/2016 0:00	2/14/2016 0:00	62.49	66.82	4.33	2.41
2/14/2016 0:00	2/15/2016 0:00	62.07	66.78	4.71	2.62
2/15/2016 0:00	2/16/2016 0:00	60.90	65.66	4.75	2.64
2/16/2016 0:00	2/17/2016 0:00	60.84	65.37	4.53	2.52

2/17/2016 0:00	2/18/2016 0:00	63.20	66.90	3.70	2.06
2/18/2016 0:00	2/19/2016 0:00	62.20	66.57	4.36	2.42
2/19/2016 0:00	2/20/2016 0:00	66.99	70.33	3.34	1.86
2/20/2016 0:00	2/21/2016 0:00	61.71	65.17	3.47	1.93
2/21/2016 0:00	2/22/2016 0:00	61.95	63.81	1.86	1.03
2/22/2016 0:00	2/23/2016 0:00	61.96	63.09	1.14	0.63
2/23/2016 0:00	2/24/2016 0:00	61.95	63.23	1.28	0.71
2/24/2016 0:00	2/25/2016 0:00	62.01	64.21	2.20	1.22
2/25/2016 0:00	2/26/2016 0:00	61.67	64.23	2.56	1.42
2/26/2016 0:00	2/27/2016 0:00	61.60	65.09	3.48	1.93
2/27/2016 0:00	2/28/2016 0:00	62.18	65.59	3.40	1.89
2/28/2016 0:00	2/29/2016 0:00	62.93	66.94	4.01	2.23
2/29/2016 0:00	3/1/2016 0:00	63.18	67.48	4.29	2.39
3/1/2016 0:00	3/2/2016 0:00	63.27	67.68	4.41	2.45
3/2/2016 0:00	3/3/2016 0:00	63.40	67.79	4.39	2.44
3/3/2016 0:00	3/4/2016 0:00	63.82	68.08	4.26	2.37
3/4/2016 0:00	3/5/2016 0:00	64.48	68.50	4.02	2.23
3/5/2016 0:00	3/6/2016 0:00	63.88	67.63	3.75	2.08
3/6/2016 0:00	3/7/2016 0:00	63.98	66.45	2.47	1.37
3/7/2016 0:00	3/8/2016 0:00	68.44	67.64	-0.80	-0.44
3/8/2016 0:00	3/9/2016 0:00	62.21	65.57	3.36	1.87
3/9/2016 0:00	3/10/2016 0:00	61.99	65.02	3.02	1.68
3/10/2016 0:00	3/11/2016 0:00	62.31	64.88	2.57	1.43
3/11/2016 0:00	3/12/2016 0:00	62.59	65.08	2.49	1.39
3/12/2016 0:00	3/13/2016 0:00	61.85	64.48	2.63	1.46
3/13/2016 0:00	3/14/2016 0:00	61.75	64.00	2.25	1.25
3/14/2016 0:00	3/15/2016 0:00	62.29	65.62	3.33	1.85
3/15/2016 0:00	3/16/2016 0:00	62.32	65.59	3.27	1.81

3/16/2016 0:00	3/17/2016 0:00	62.54	66.83	4.29	2.38
3/17/2016 0:00	3/18/2016 0:00	63.07	67.79	4.73	2.63
3/18/2016 0:00	3/19/2016 0:00	64.49	69.40	4.91	2.73
3/19/2016 0:00	3/20/2016 0:00	63.91	68.55	4.64	2.58
3/20/2016 0:00	3/21/2016 0:00	63.40	65.26	1.85	1.03
3/21/2016 0:00	3/22/2016 0:00	63.41	65.25	1.84	1.02
3/22/2016 0:00	3/23/2016 0:00	63.48	64.83	1.35	0.75
3/23/2016 0:00	3/24/2016 0:00	62.51	63.21	0.69	0.39
3/24/2016 0:00	3/25/2016 0:00	60.93	62.51	1.58	0.88
3/25/2016 0:00	3/26/2016 0:00	62.27	63.07	0.80	0.44
3/26/2016 0:00	3/27/2016 0:00	61.52	65.00	3.48	1.93
3/27/2016 0:00	3/28/2016 0:00	62.12	64.90	2.79	1.55
3/28/2016 0:00	3/29/2016 0:00	62.76	64.60	1.84	1.02
3/29/2016 0:00	3/30/2016 0:00	62.09	64.46	2.37	1.32
3/30/2016 0:00	3/31/2016 0:00	61.93	64.92	2.99	1.66
3/31/2016 0:00	4/1/2016 0:00	62.43	62.30	-0.13	-0.07
Average				2.74	1.96